

UNCLASSIFIED

AD 409 620

DEFENSE DOCUMENTATION CENTER

FOR

SCIENTIFIC AND TECHNICAL INFORMATION

CAMERON STATION, ALEXANDRIA, VIRGINIA



UNCLASSIFIED

NOTICE: When government or other drawings, specifications or other data are used for any purpose other than in connection with a definitely related government procurement operation, the U. S. Government thereby incurs no responsibility, nor any obligation whatsoever; and the fact that the Government may have formulated, furnished, or in any way supplied the said drawings, specifications, or other data is not to be regarded by implication or otherwise as in any manner licensing the holder or any other person or corporation, or conveying any rights or permission to manufacture, use or sell any patented invention that may in any way be related thereto.

AMRL-TDR-63-23

409620

409 620

DEVELOPMENT AND TEST OF THE BELL ZERO-G BELT

TECHNICAL DOCUMENTARY REPORT NO. AMRL-TDR-63-23

March 1963

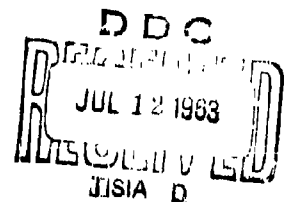
Behavioral Sciences Laboratory
6570th Aerospace Medical Research Laboratories
Aerospace Medical Division
Air Force Systems Command
United States Air Force
Wright-Patterson Air Force Base, Ohio

Contract Monitor: Donald D. Mueller, Capt, USAF
Project No. 7184, Task No. 718405

[Prepared under Contract No. AF33(657)-9224

by

Ralph E. Flexman
Leonard M. Seale
Campbell Henderson
The Bell Aerosystems Company
Buffalo 5, New York]



NOTICES

When US Government drawings, specifications, or other data are used for any purpose other than a definitely related government procurement operation, the government thereby incurs no responsibility nor any obligation whatsoever; and the fact that the government may have formulated, furnished, or in any way supplied the said drawings, specifications, or other data is not to be regarded by implication or otherwise, as in any manner licensing the holder or any other person or corporation, or conveying any rights or permission to manufacture, use, or sell any patented invention that may in any way be related thereto.

Qualified requesters may obtain copies from ASTIA. Orders will be expedited if placed through the librarian or other person designated to request documents from ASTIA.

Do not return this copy. Retain or destroy.

Stock quantities available at Office of Technical Services, Department of Commerce, \$2.50.

Change of Address

Organizations receiving reports via the 6570th Aerospace Medical Research Laboratories automatic mailing lists should submit the addressograph plate stamp on the report envelope or refer to the code number when corresponding about change of address.

FOREWORD

This study was monitored by the Behavioral Sciences Laboratory of the 6570th Aerospace Medical Research Laboratories, Aerospace Medical Division, Wright-Patterson Air Force Base, Ohio. The technical work described in this report was by the Bell Aerosystems Company, Buffalo 5, New York, under Contract AF33(657)-9224. Mr. Ralph E. Flexman was principal investigator for Bell Aerosystems Company. Captain Donald D. Mueller of the Crew Stations Branch, Human Engineering Division, was the contract monitor for the 6570th Aerospace Medical Research Laboratories. The work was performed in support of Project No. 7184, "Human Performance in Advanced Systems" and Task No. 718405, "Design Criteria for Crew Stations in Advanced Space Systems." The work specific to this contract was initiated in July 1962 and completed December 1962.

The authors wish to acknowledge the valuable work contributed by Mr. Wendell Moore, special project engineer, Bell Aerosystems Company (for his work on the SRLD). Particular appreciation is expressed to Captains John Simons, Melvin Gardner, and Donald D. Mueller of the Aerospace Medical Research Laboratories.

This report is cataloged as Bell Aerosystems Report Number D7123-953002.

ABSTRACT

The assumption is made that a requirement exists for the development of a self-maneuvering system for orbital workers. Such a system will consist of a life support subsystem, maintenance equipment (tools), and a propulsion and control subsystem. This report discusses the general problem areas and specifically reports on the research, development, and testing of the Bell Zero-G Belt, a research propulsion and control system for maneuvering a man in a weightless environment. The flight tests of the belt took place on a large airbearing platform and in a C-131 cargo-type aircraft during zero-g trajectories. The equations of motion derived during the Bell Aero-systems Company sponsored development of the Small Rocket Lift Device (Rocket Belt) are also presented and discussed with respect to the Zero-G Belt. Specific conclusions are presented on the adequacy of the research model of a propulsion system and recommendations are made for additional research and development.

PUBLICATION REVIEW

This technical documentary report has been reviewed and is approved.

Walter F. Grether

WALTER F. GREETHER
Technical Director
Behavioral Sciences Laboratory

CONTENTS

Section	Page
I INTRODUCTION	1
II CONCEPT DEVELOPMENT	6
III DESIGN AND DEVELOPMENT OF THE SRLD	12
A. Damping Analysis	25
B. Open Loop Analysis	37
C. Closed Loop Analysis	42
D. Analog Computer Study of Open and Closed Loop	45
IV DEVELOPMENT OF THE ZERO-G BELT	53
V HARDWARE DEVELOPMENT PROGRAM	61
A. Corrosion and Rust Inhibiting	68
B. Assembly	70
VI ZERO-G BELT TEST AND EVALUATION	73
A. Air Bearing Platform Tests	73
B. Flight Tests	76
VII CONCLUSIONS	88
VIII RECOMMENDATIONS	90
A. Maintenance Task Parameters	90
B. Orbital Worker Control Capabilities	92
C. Environment Parameters	93
D. Stability, Control, and Propulsion Concepts	93
E. Approaches to Study	94
1. Water Immersion	94
2. Three-Degree-of-Freedom Air Bearing Device	94
3. Keplerian Trajectories	95
4. Improved Simulation Approaches	95
IX REFERENCES	96
APPENDIX Simplified Equations of Motion for SRLD-Uncontrolled ..	98

ILLUSTRATIONS

Figure		Page
1	Encapsulation Concepts for the Orbital Environment	2
2	Stabilization and Control Systems	4
3	Zero-G Space Belt in Position	9
4	Zero-G Space Belt	10
5	Detail of Thrust Controller Unit	11
6	First Model of the SRLD	13
7	Flight Tether in Operation	14
8	An Early Free Flight	15
9	Photoschematic-Propulsion System	16
10	One-G Rocket Belt Test Facility	18
11	Lateral Period of Lift Device (and Man) for Various Control Ratios and Control Arms	23
12	Preferred Control Systems - SRLD	24
13	Simplified Rigid Body Model for Damping Analysis	26
14	Possible Control Schemes	29
15	Manual Control and Damping by Natural Reaction	31
16	Semimanual Damping	32
17	Automatic Damping System	33
18	Artist's Concept of Small Rocket Lift Device	35
19	Schematic of Stability Augmentation Device	36
20	Schematic Representation of Man-Machine Combination	38
21	Body Frequency versus Hip Spring Stiffness (Tanks Full)	39
22	Root Loci	44
23	Analog Computer Diagram	46
24	Analog Computer Results	47
25	Analog Computer Results	48
26	Analog Computer Results	49
27	Analog Computer Results	50
28	Analog Computer Results	51
29	Analog Computer	52
30	Functional Block Diagram of the Stability and Control System	54
31	Two-Segment Body Model	56
32	Oscilloscope Display Schematic	59
33	Analog Flight Simulator	60
34	Zero-G Belt Schematic	62
35	Top View of Thrust/Control Assembly	64
36	End View of Thrust/Control Assembly	65
37	Tube Bundle Assembly with Low Pressure Tubes Separated	66

ILLUSTRATIONS (CONT)

Figure		Page
38	Complete Tube Bundle Assembly	67
39	Test Tubes Showing high Pressure Rupture	69
40	Front View of the Zero-G Belt	71
41	Rear View of the Zero-G Belt	72
42	The Bell Air Bearing Platform	74
43	Zero-G Belt Training on the Air Bearing Platform	75
44	Thrust Testing of the Air Bearing Platform	77
45	Close-up of Thrust Testing Rig	78
46	Zero-G Belt in Flight	82
47	Orbital Worker Systems Study Plan	91
48	Torso Reference Data	102

TABLES

Number		Page
I	Weight Estimate SRLD, Monopropellant H ₂ O ₂	40
II	Numerical Values of Man-Machine Parameters	41
III	Thrust Levels Measured on the Zero-G Belt	79
IV	Maneuver Schedule for Zero-G Belt Flight Test	81
V	Zero-G Belt Flight Test Record	83
VI	Maneuver and Scoring Instructions	84
VII	Estimated Percent Success of Each Maneuver	85
VIII	Mean Operator Ratings of Each Maneuver Component	86
IX	Performance Ratings on the Zero-G Belt	87

SECTION I. INTRODUCTION

Man's role in operational space systems will sooner or later require him to perform tasks external to his space vehicle. Anticipating this requirement, the Bell Aerosystems Company initiated, in 1959, a program of study and development on systems necessary to support and augment an orbital worker's basic capabilities. This program considered that the configuration of an orbital worker system could vary from the simplest, a full pressure suit with the required life support, propulsion and stabilization systems integrated into it, to the more complex, a rigid structure encapsulating the man and including a well integrated distribution of the required subsystems. These two extreme forms of encapsulation are depicted in Figure 1, which shows orbital workers in pressure suits and workers encapsulated in a nonanthropomorphic capsule called REMORA (1).

The program pursued by Bell assumed that system requirements existed for both systems, and therefore, engaged in studies of both systems. This report discusses the work leading up to the development of a Zero-G Belt, the flight testing of the belt and the conclusions and recommendations resulting from this effort.

It should be emphasized that Bell has conducted extensive analyses of the orbital worker propulsion system over and above those presented in this report. These studies have been directed toward the design of an operational backpack system including propulsion, stabilization and control, and life support system. These studies have resulted in the preliminary design of this system.

The basic assumption on which the Bell program has been based may be stated as follows:

The requirement exists for the astronaut to engage in useful activities outside of his vehicle in both the orbital and planetary environments. These activities will range from emergency egress from his mother ship to translation to another vehicle, for conducting maintenance, repair, and assembly functions in space. Such activities require the joint development of systems capable of sustaining life in the predicted environments and systems capable of translating the astronaut limited distances with stability, control, and minimum expenditure of propulsive power and life support system constituents.

To satisfy the requirements of this assumption, expanded research activities must be undertaken in a number of areas centered around the man's capability to maneuver, with control, in environments of modified gravitational fields. Studies of this nature will be concerned with the following three major subsystems which comprise the orbital worker self-maneuvering system:



Figure 1. Encapsulation Concepts for the Orbital Environment

- (a) Life support system
- (b) Support equipment (tools and other equipments necessary for the successful completion of orbital maintenance activities)
- (c) Propulsion, stability and control system

It must be recognized that the efficient development of an orbital worker system requires an integrated engineering study of each of these areas. However, this report is restricted to a discussion of some of the Bell Aerosystems Company sponsored research on the analysis and design of the propulsion and stabilization and control systems, and discusses the results of test work completed with a prototype system, the Zero-G Belt.

The work summarized in this report was initiated during mid-year 1959 and was completed in November 1961. Subsequent to the latter date Bell has completed extensive design analyses of operational back-pack propulsion systems including mono-propellant, bipropellant and gas storage systems. In addition to these system studies others have been completed of the stabilization and control system, rendezvous maneuvers and life support system integration (1-4). These Bell Aerosystems Company sponsored studies are considered outside the scope of the present contract and are not presented in this report. For a similar reason the results of the recently completed USAF sponsored studies are not included in this report.

Figure 2 illustrates the system concepts which have been studied for translational and rotational control of the orbital worker. These systems encompass the stabilization spectrum from completely manual to automatic.

By a completely manual system we mean one in which the controlled quantities (rotational and translational position, rate or acceleration) are sensed by the human and the control inputs to the propulsion system are made through pilot initiated control movements without the assistance of a stabilization augmentation system. The automatic systems are those in which the command inputs are pilot initiated but are maintained at the commanded value (plus or minus a system threshold error) by automatic sensors and propulsion system actuators.

Figure 2 does not represent all possible system configurations, as combinations of two or more systems may offer enhanced stabilization. For example, a manual translational control system may be combined with an automatic angular rate control system. It should be noted, however, that even in automatic systems the command inputs in terms of rate or position are pilot initiated. Therefore, the function of the automatic system is to maintain the commanded value of position or rate; that is, stabilization is provided by a simplified closed loop operation which uses the man to close the loop.

The primary parameter which defines the dynamic response characteristics of the Zero-G Belt is the location of the center of mass of the system relative to the point of application of a produced torque or moment. The use of the full pressure suit, with its flexibility (even though limited), presents some problems in this regard. For example,

System	Controlled Quantity		Typical Sensors		Control Force	
	Rotation	Translation	Rotation	Translation	Rotation	Translation
I	Attitude	Position	Human	Human	Arms, Legs, Torso	Propulsive
II	Attitude	Position	Human	Human	Propulsive	Propulsive
III	Rate	Velocity	Rate Gyros	Accelerometers	Propulsive	Propulsive
IV	Rate and Attitude	Acceleration Velocity Position	Position and Rate Gyros	Accelerometers	Propulsive	Propulsive
V	Attitude	Acceleration Velocity Position	Human	Accelerometers	Gyroscope	Propulsive

Figure 2. Stabilization and Control Systems

any time the man repositions one of his appendages or lifts a tool or some other object, the location of the center of mass will change. The application of a reaction control force at such times will result in a thrust vector displaced from the center of mass and will result in a rotation of the orbital worker. Such undesired rotations must be controlled either by direct manual control or through the use of one of the various automatic systems described above.

SECTION II. CONCEPT DEVELOPMENT

The requirement for a personal propulsion system to permit an astronaut to move about in the weightless environment of outer space was recognized quite early at the Aerospace Medical Laboratory.* In February of 1958, they initiated a research program to study the effects of zero gravity on human performance and to explore the necessary characteristics of a propulsion system for a free floating man. The sub-gravity environment for their studies was provided by flying a cargo type aircraft through a Keplerian trajectory. The aircraft first used was a C-131 transport that had been modified to withstand the unique stresses that occur when producing zero gravity in this manner. By flying the C-131 through the maneuver at its maximum safe limits, a period of weightlessness of approximately 15 seconds was experienced. Additional modifications of the aircraft made it possible for a subject to free float and maneuver in a padded area of the cabin that was 8 feet wide, 25 feet long and 6 feet high.

Although the work of the Aerospace Medical Laboratory covered a wide range of zero-g experiments, their work on several rudimentary propulsion systems was of particular relevance to the development of the Bell Zero-G belt. The first system tested was a single jet propulsion unit designated the "Mark I". The unit consisted of 6 high pressure "bailout" bottles fastened together and attached to a pressure reduction system. A 1/8 inch, high pressure line attached the pressure reduction system to a nozzle that was controlled by a simple trigger. The working pressure of 400 to 600 psig gave a thrust of approximately three pounds. Flight tests of the device proved that the thrust was too low to be useful for maneuvering in the 15-second test period. However, experience with the unit did indicate the importance of accurately aligning forces through the center of mass of the man when straight line translations were attempted.

The second system to be tested, the "Mark II", was likewise a single nozzle unit. It consisted of a high pressure bottle and a special pistol shaped unit combining the thrust nozzle and its controller. The nozzle was attached to the bottle by a length of high pressure, flexible tubing. The Mark II had a working pressure of 1800 psig and produced a thrust of 15 to 17 pounds. Flight tests also proved this unit inadequate. When the hose was pressurized, it became too stiff to allow accurate alignment of the thrust or to turn the nozzle with a single hand. However, the amount of thrust appeared to be adequate for translation even though uncontrolled rotation frequently occurred when the nozzle was moved just a few inches from direct alignment with the operator's center of mass. Yet, several straight line translations were successfully made.

At this point, just after testing the Mark II unit, an exchange of technical information between Bell and the Air Force took place. On the one hand, Bell was

* The name of the Aerospace Medical Laboratory has been changed to the 6570th Aerospace Medical Research Laboratories.

carrying on a company sponsored development of a rocket belt that would permit a man to free fly in a one-g environment and the Air Force a program to develop a system that would permit man to fly in a zero-g environment

The Bell program consisted of certain theoretical and computer studies, simulator tests, design studies, subsystem tests, and tethered flights with a compressed nitrogen system. The validity of this development effort was soon demonstrated by a number of successful free flights with a completely functional rocket belt. The results of this work provided important information on the equations of motion of a free flying man, the spring constants of a human body, the optimum location of thrust units with respect to a man's center of mass, and the stability and control requirements of a man-propulsion system. Since this information had direct application for establishing design parameters of a zero-g propulsion system, a fairly extensive description of the basic work done by Bell on the SRLD is presented in the next section.

The relevance of the rocket belt work to the problems of manned flight under zero-g spurred a company decision to extend its man-propulsion system work to include the development of a Zero-G Belt. Criteria for a propulsion system of this type was tentatively defined by discussions with the Air Force and through other conceptual analyses of the problem area. Although an ultimate space system was envisioned, it became quite obvious that the immediate requirement was for an interim or research unit that could be used in the cabin of the C-131 when subgravity producing parabolas were flown. The essential characteristics for a satisfactory test unit were assumed to include:

- (1) The thrust units should be located so that all translational forces would be either through the center of mass of the operator or at his cg level with paired thrust on each side of the cg axis.
- (2) Location of the thrust units for controlling rotation about any of the three axes should make a lever arm appropriate to the amount of thrust being generated to produce a controllable rate of rotation.
- (3) The propulsion unit should be capable of producing a sustained thrust of 15 pounds.
- (4) The control system should be simple, utilize natural movements, and be instantaneously responsive.
- (5) The exhaust products of the propulsion system should be neither toxic nor dangerous, nor otherwise incompatible with an aircraft environment.
- (6) If a high pressure, cold gas system was used as a propellant, adequate safeguards had to be incorporated into the design to prevent injury to the operator in the event of structural damage due to a hard fall or contact.

- (7) The total weight of the system to be carried by the operator should be as light as possible and not exceed 65 pounds.

Utilizing these criteria for establishing a preliminary concept, in September of 1959 a Bell design was formulated and a patent application submitted (patent was issued on December 4, 1962). Figures 3, 4, and 5 present an artist's concept of the original design. An engineering design program was initiated shortly thereafter, but actual construction of a test unit was not started until December of 1960. The initial unit, Bell Model 8170, was completely assembled and functionally tested in March, 1961. First flight testing of the belt under conditions of zero gravity took place in April, 1961, and utilized the Aerospace Medical Laboratory's C-131 aircraft.

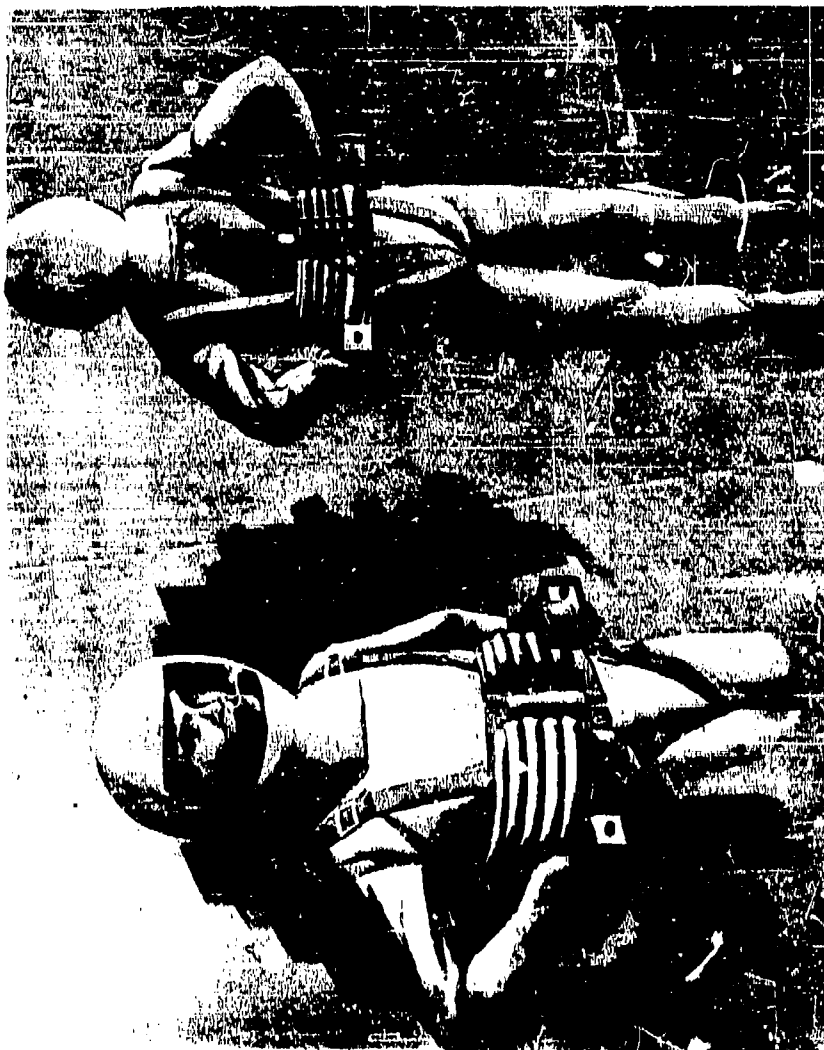


Figure 3. Zero-G Space Belt in Position



Figure 4. Zero-G Space Belt

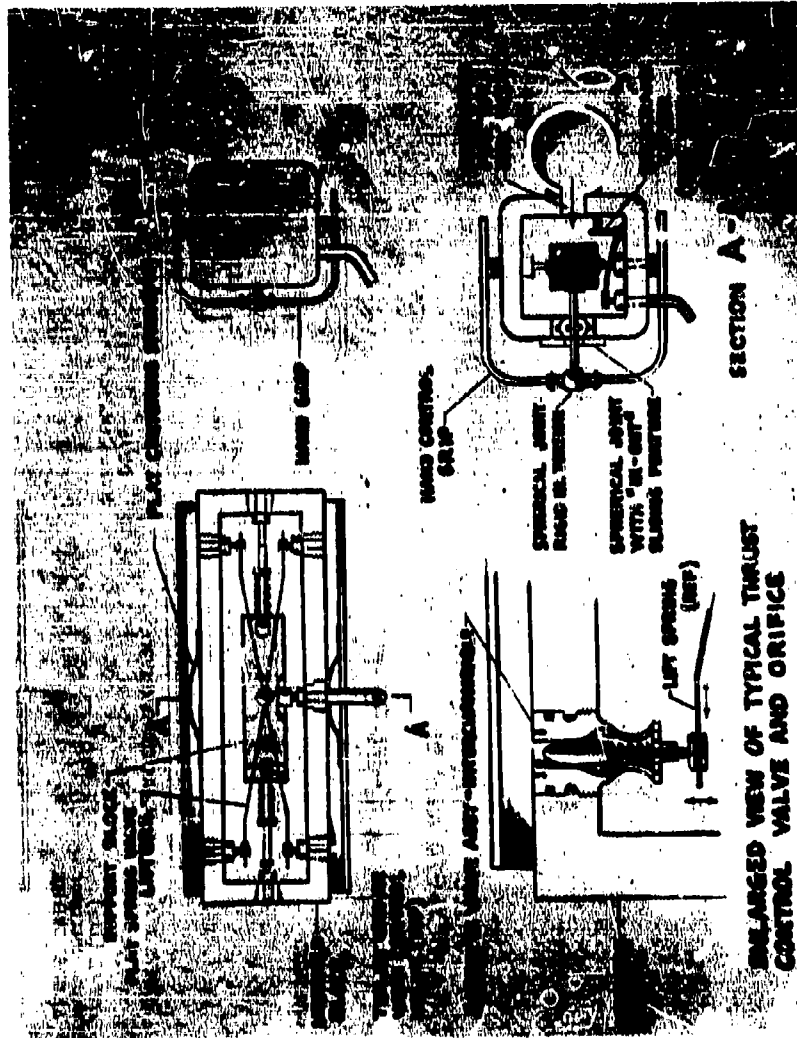


Figure 5. Detail of Thrust Controller Unit

SECTION III. DESIGN AND DEVELOPMENT OF THE SRLD

As discussed in the previous section, the immediate predecessor of the Bell Zero-G Bell was Bell's SRLD (Small Rocket Lift Device, popularly called the rocket belt). The SRLD had its genesis in the first rocket plane to be built and flown in this country, the Bell X-1A. Early in the development of this aircraft, the requirement for additional control forces was recognized and led to the development of a hydrogen peroxide reaction control system. Experience with the small rocket motors of this system suggested the technical feasibility of achieving a manned rocket flight by attaching motors of this type directly to a man's body. The first design of such a system was conceived in 1953 and added a new dimension to the realm of flight by a successful free flight on 20 April 1961. Figure 6 shows the first model of the SRLD. It should be pointed out that a number of significant changes have since been made in the configuration of the SRLD. Figure 7 is a picture of the unit being flown in the tethering rig. Figure 8 shows the SRLD in one of its first free flights.

The SRLD is a pressurized hydrogen peroxide propulsion system capable of producing 300 pounds of thrust. It is mounted on a fiberglass corset molded to fit the operator's body. Two handles, attached to underarm lift rings through a central lateral pivot point, provide a motorcycle type throttle on the right and a yaw control on the left. All other control of the system is generated kinesthetically by the operator's body. Two rocket nozzles, one on each side, mounted outboard of the arms and above the center of gravity, provide the actual lift. The nozzles are fed by a gas generator, controlled by the hand throttle. Over 300 successful flights have been accomplished demonstrating the reliability of the system and its capability. Thus far, maneuvers such as straight and level flight from point to point, coordinated and precise turns, hovering, hill climbing and descents, over water and various physical barriers have been demonstrated.

In its present configuration, the device is considered to be a feasibility or research item. Its objectives have been to demonstrate the use of a rocket propulsion system, carried on a man's back, to translate him over the earth's surface in controlled flight.

Figure 9 is a model schematic of the SRLD. As depicted, the SRLD is a hydrogen peroxide propulsion system that is nitrogen pressurized. The nitrogen bottle is charged through a standard aircraft fill valve to a pressure of 3000 psi. Pressure is indicated by a miniature high pressure gauge. Gas flow is controlled by a manually operated N₂ shutoff valve developed for the Mercury Program. This is followed by a 10-micron filter which flows into a pressure regulator. A check valve is provided which prevents backflow of H₂O₂. Pressure to and from the propellant tankage is manually controlled by a "pressure and vent" 3-way valve. A 0-800 psi tank pressure gauge is tied in just downstream of the pressure and vent valve along with the relief valve.

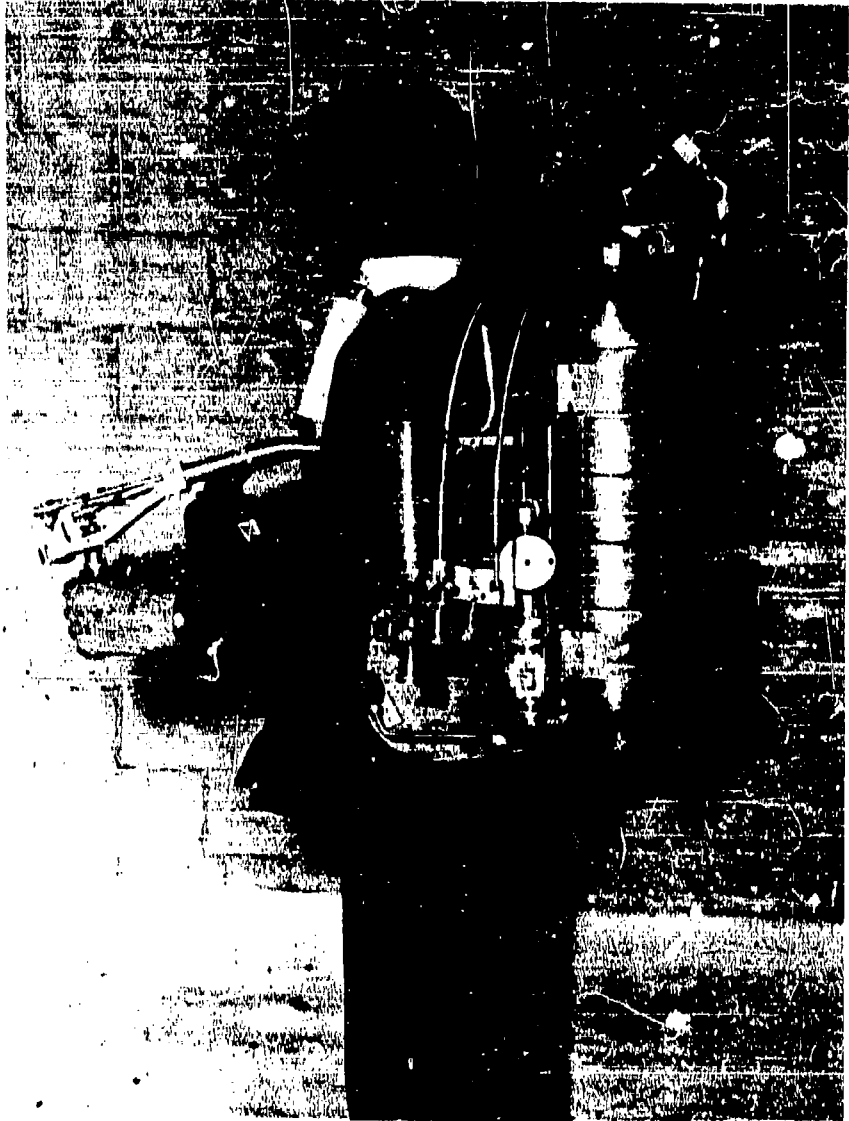


Figure 6. First Model of the SRLD



Figure 7. Flight Tether in Operation



Figure 8. An Early Free Flight

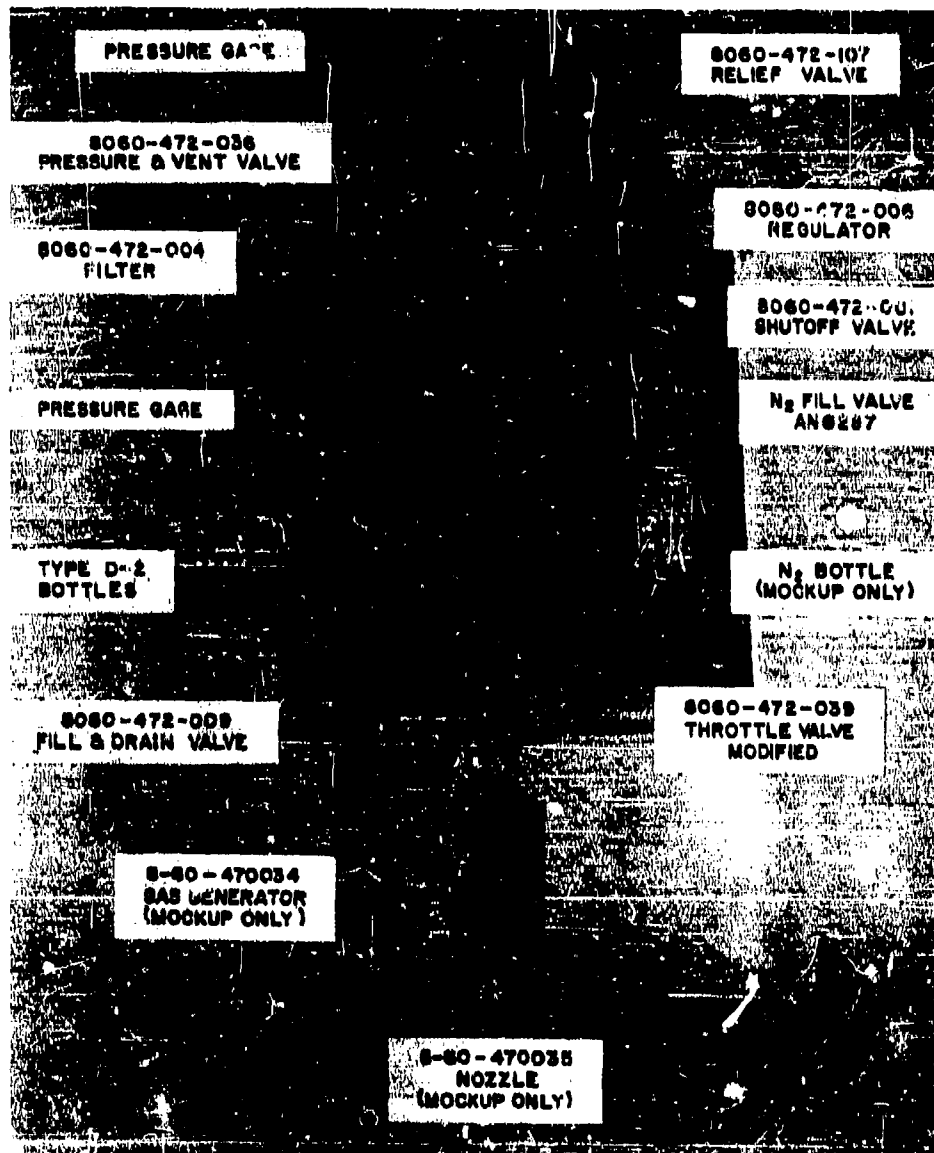


Figure 9. Photomicrograph-Propulsion System

The propellant tankage consists of two modified AF type D-2 breathing oxygen bottles tied together by special bosses. A small shutoff valve is located at one end of the manifold and a tank bleed valve is provided. Overflow tubes are inserted at a predetermined height. Propellant flows under a pressure of 450 psi from the manifold to the throttle valve. The throttle valve varies the hydrogen peroxide flow to the gas generator from zero to maximum. The peroxide is decomposed by catalytic action in the gas generator, employing a silver screen catalyst. The decomposed gases are directed through, and expanded in, the two exhaust nozzles to produce throttleable thrust.

Specifications of the system are:

Propellant	Hydrogen Peroxide (90%)
Empty weight	54 lb
Propellant weight	47 lb
Operator weight	175 lb
Takeoff weight	276 lb
Usable duration	26 sec
Maximum Range (Horizontal)	1420 ft
Maximum Altitude (Vertical Ascent)	996 ft
Maximum Altitude (Vertical Descent)	2000 ft
Maximum Altitude (Vertical Ascent and Descent)	324 ft

The development history of the SRLD began in 1953 with several informal design studies. However, it was not until 1958 that a specific program was initiated. Of particular relevance to the Zero-G Belt is the development testing that was done on a nitrogen propulsion unit, the studies accomplished on a REAC simulator, and various dynamic analyses.

The first man-lift device built by Bell was flown by several people (under controlled conditions) to determine feasibility of the rocket belt concept. The rig incorporated two fixed rocket nozzles extending laterally from a shoulder harness, which under hovering conditions provide a thrust equal to the man-plus-rig weight. In the test rig, thrust was developed from high pressure nitrogen supplied from an external source through a flexible hose to the rocket nozzles. Figure 10 shows this test rig in action. Hovering flights of short duration were accomplished with some short fore, aft, and lateral translations. In most of the early tethered flights on this rig, an uncontrollable lateral oscillation developed which required termination of the flight. For this reason, an analytical study of the stability and control characteristics of the proposed rocket belt was made to determine what design modifications could be made to insure an acceptable system from a stability and control standpoint. Due to the complexities involved in completely simulating human torso dynamics, a simplified mathematical model was used in this analysis. The objectives of the analysis were to:

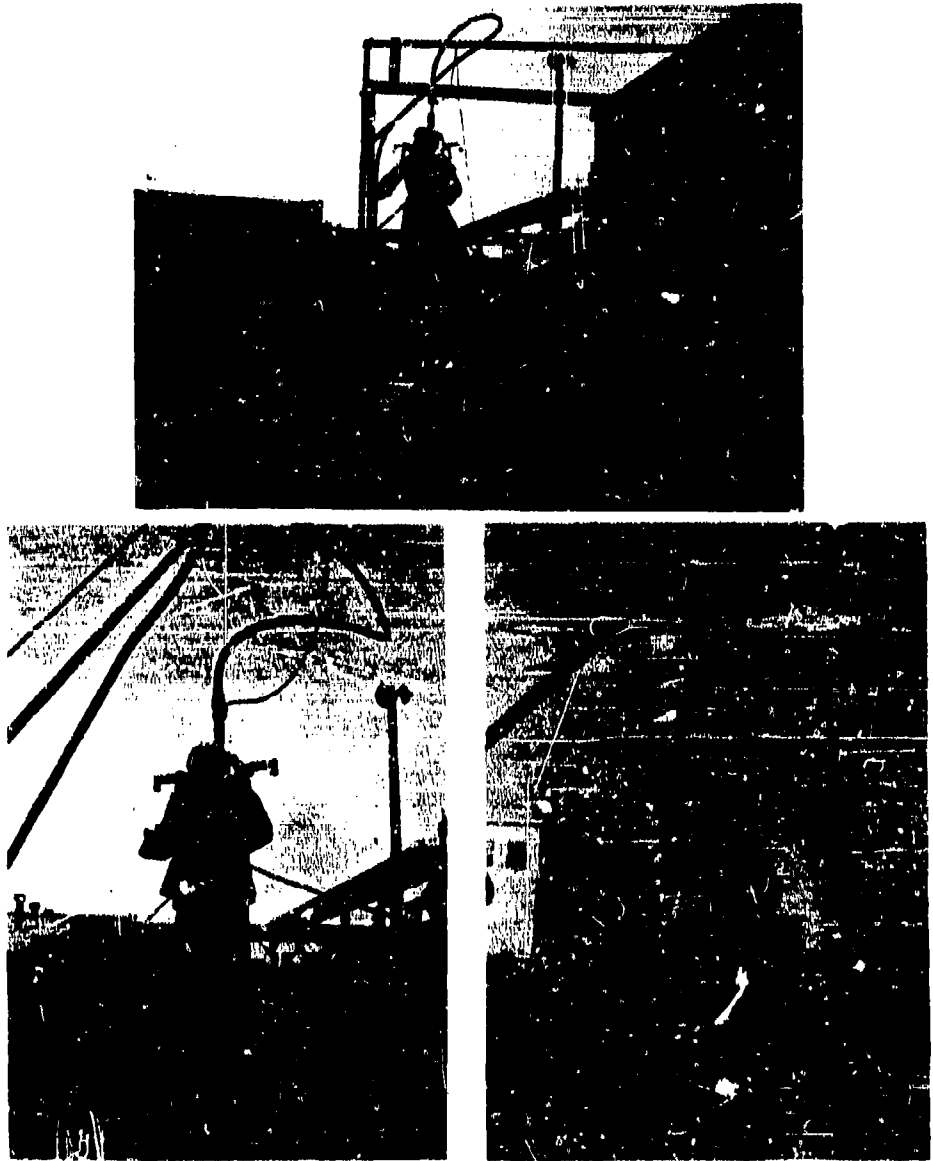
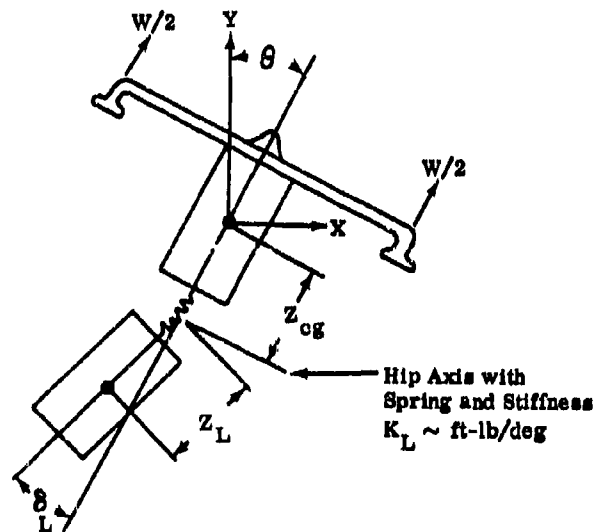


Figure 10. One -G Rocket Belt Test Facility

- (1) Solve the equations of motion for the simplified model to determine their validity in predicting observed motions and if so, to evaluate the parameters that affect stability.
- (2) Incorporate into the equations a thrust vector control function, both with and without damping. Evaluate numerically the parameters involved that affect stability and control.
- (3) Determine practical design modifications which would achieve desired values of the parameters determined, e.g., torso orientation and support, control locations and deflections, damping ratios (and methods) etc.
- (4) Study qualitatively techniques to obtain center of gravity control (with fixed nozzles) which takes advantage of natural reactions.
- (5) Recommend preferred systems and alternates.

The lateral equations of motion were solved for the nitrogen rig and simplified as shown in the sketch below.



The upper torso is considered rigid, with nozzles rigidly attached. The lower extremity (below hip axis) is considered to be attached to the upper torso by a spring of stiffness K_L . The solution of the equations of motion (details are given in Appendix A) show that, once started, the system will translate from side to side through excursions of X and rotate through excursions of θ , both at the same frequency (the legs swing as pendulums at the same frequency). The frequency of oscillation was found to be,

$$\omega \approx \sqrt{\frac{W_L^2 Z_L}{57.3 I (K'_L)}} \text{ rad/sec}$$

The amplitude ratios are,

$$\frac{\theta_{\max}}{\theta_0} = 1 \text{ and } \frac{x_{\max}}{\theta_{\max}} \approx \frac{I K'_L}{W_L^2 Z_L} g$$

where W_L = Weight of lower extremity, lb

Z_L = Distance shown in sketch, ft

K_L = Hip axis spring stiffness, ft-lb/deg

$K'_L = (K_L/Z_L + W_L/57.3)$

I = Total moment of inertia about system cg, slugs ft²

Note: Vertical motions were not considered.

Using torso data for an average man, the frequency and period of the system were found to be,

$$\omega = 1.7 \text{ rad/sec}$$

$$T = 3.7 \text{ sec}$$

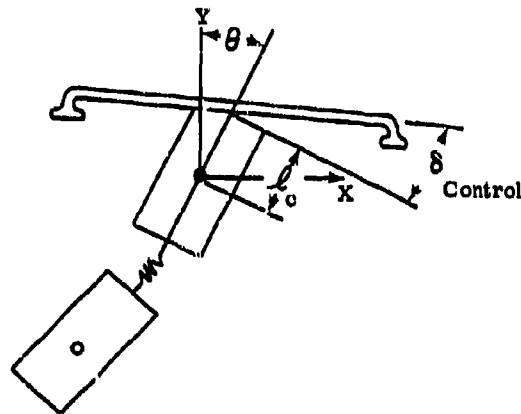
The amplitude ratio, $x_{\max}/\theta_{\max} = 0.19 \text{ ft/deg}$

These values compared reasonably well with the observed values in the test rig. The time history solutions however, indicated that an oscillation, once started, will persist at a constant amplitude, while in actual tests amplitudes appeared to increase with time. It was felt that the increasing amplitudes observed in tests were operator induced.

As seen from the equations, there are two variable design quantities which can produce longer periods, Z_L and K_L ; i.e., lower values of Z_L (legs retracted) and/or higher values of K_L (hip axis stiffness). Because of the agreement between analytical results and observed test results, the simplified model was used as the basis for analysis and evaluation of design modifications. It is to be noted that the location of the support point has no significance from this analysis.

Another observation from the test flights was that to control all disturbances and move directionally, it was necessary to deflect the thrust vector relative to the body. This was done in the test rig by forcibly rotating the harness relative to the shoulders. Attempts to control movements by deflecting arms or legs (cg control) usually started oscillations which could not be stopped by leg or arm movements.

The effect of adding thrust vector control (deflectable nozzles or jetavators) was analyzed by including in the equations of motion a proportional control term $K = \delta_{\text{control}}$. This can be physically accomplished by providing a control stick attached to the nozzles, with which the operator can deflect the nozzles in proportion to his angular orientation. A value of $K = 1.0$ implies that he hold his stick (and nozzles) in one fixed orientation relative to the ground such as perpendicular to the ground to arrest disturbances. The model used in the analysis was the same as sketch presented earlier with the addition of deflectable nozzles (see sketch below).



Solutions of the equations of motion with control (see Appendix A) show the following frequency and amplitude ratios,

$$\omega^2 = \frac{W_L^2 Z_L (1-K)}{57.3 K_L I} + \frac{l_c K W}{I}$$

$$\frac{\theta_{\max}}{\theta_0} = 1$$

$$\frac{x_{\max}}{\theta_0} = \frac{I K_L g (1-K)}{W_L^2 Z_L (1-K) + W l_c K K_L 57.3}$$

where K = Control gain ratio

l_c = Distance between control swivel point and system center of gravity

$$K'_L = (K_L/Z_L + W_L/57.3) = \text{lumped stiffness parameter}$$

These equations reduce to the same as those for the uncontrolled case when $K = 0$.

The period of oscillation $T = \frac{2\pi}{\omega}$ has been evaluated numerically (torso data for an average man) for a range of the variables for which design modifications are possible; i.e., K , Z_L , K_L , ℓ_C , and the results are plotted in Figure 11. It was assumed that improved stability and controllability should result if the period of oscillation T were increased, the lateral excursions X_{\max}/θ_{\max} would decrease, and if in addition, the simple control function (holding the stick in a nearly fixed orientation relative to the ground was incorporated). How effectively a man can hold the control stick in or close to such a position could only be evaluated experimentally. The solid lines in the figure show the effect of varying control gain ratio K and control arm ℓ_C , with nominal values of K'_L (taken to be 1.0) and $Z_L = 15$ inches. It is seen that the period increases with decreasing ℓ_C and decreasing K . The effects of decreasing Z_L to 7.5 inches (legs retracted) with an associated increase in $K'_L = 4.0$ (attributable to greater muscular rigidity) are shown by the dashed lines for the two lower values of ℓ_C . The other line shows the effect of increasing K_L essentially to ∞ .

The combined effect of reducing control arm ℓ_C to about 5 inches, reducing Z_L and increasing K'_L will produce higher periods, particularly for lower values of the control gain ratio K . It is felt that a value of $\ell_C \approx 5$ inches (for an average man) should be used to prevent the control arm from becoming negative for short stature operators. Lowest possible values of Z_L should be used, implying a provision in the rig to support the legs close to the upper torso, and/or highest practical values of K_L (hip axis stiffness) should be incorporated.

This could be accomplished at least partially by providing foot supports that are rigidly attached to the rest of the rig. A low value of K (about 0.2) also appears desirable and can be attained by incorporating a maximum deflection limit, say 3° . Then, reduced gain ratios automatically result when disturbance oscillations are large (due to gusts, etc.). For smaller disturbances and inadvertent stick motion, low gain ratios can also be achieved by designing a high gear ratio between stick deflection and nozzle deflection.

All the above design considerations were intended to produce a system that facilitates control, and permits the pilot to control oscillations (due to disturbances and inadvertent control motions) to a low value. The operator's control function is a simple one; namely to hold his stick vertical for hovering flight and to hold it aligned with his body axis for translational flight.

A sketch of a preferred control system (damping system not included) is shown in Figure 12. Methods of incorporating damping are discussed and shown in the following section.

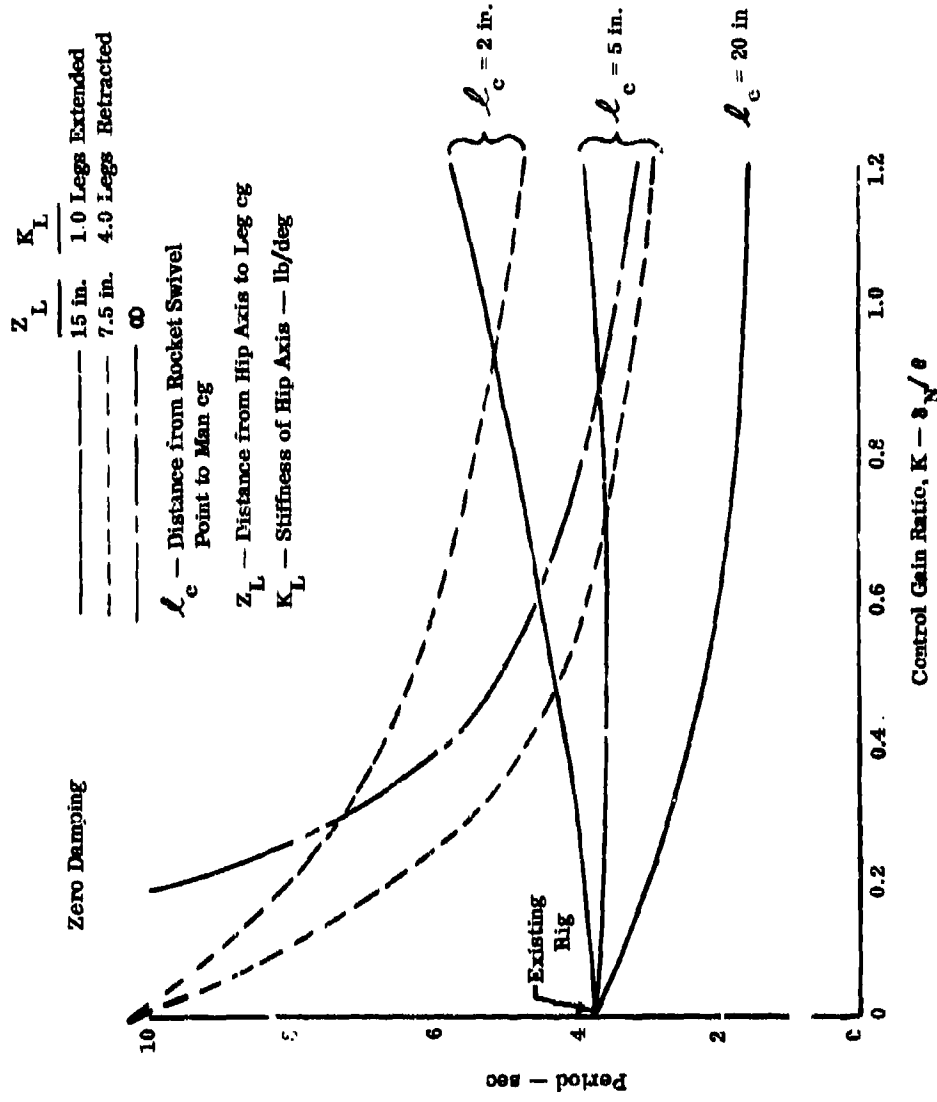


Figure 11. Lateral Period of Lift Device (and Man) for Various Control Ratios & Control Arms

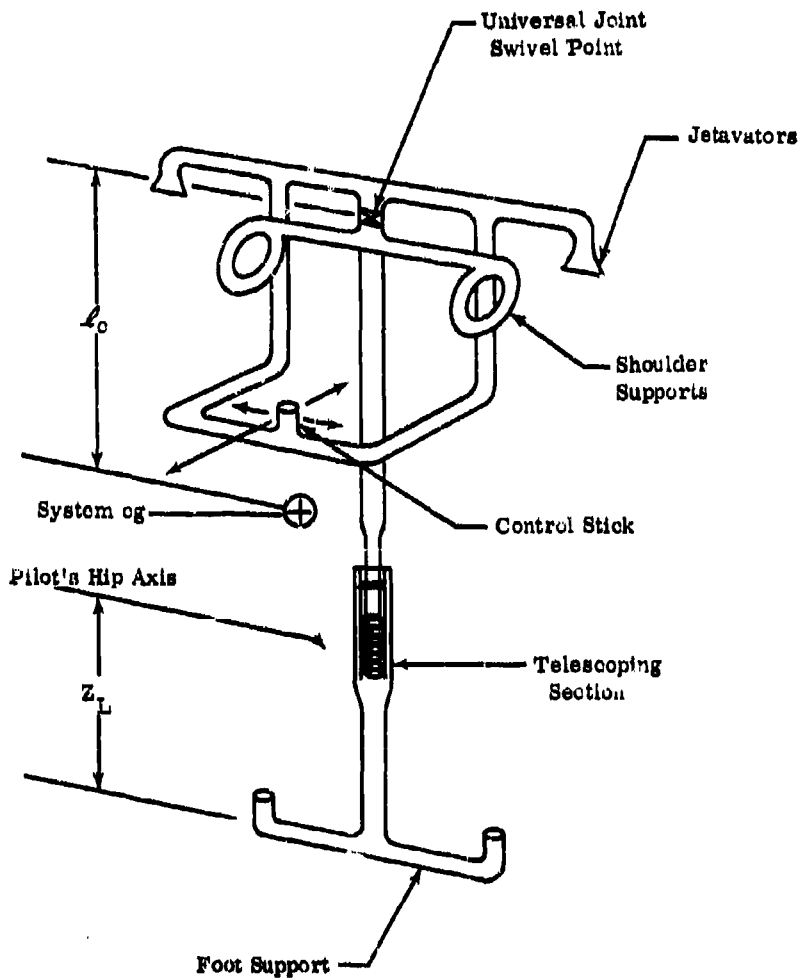


Figure 12. Preferred Control System PRLD

The desired design features are:

- (1) Deflectable nozzles by method of universal joint shown in Figure 19 or use of jetavators.
- (2) Distance from nozzle swivel point to complete system center of gravity $L_c = 5$ inches.
- (3) Nominal (undeflected) thrust vector acts through system center of gravity.
- (4) Thrust vector deflection limit approximately 3° . Deflection limit should be a variable for test purposes.
- (5) Control stick conveniently located.
- (6) A telescoping foot support which holds the man's legs retracted.
- (7) Length of foot support such that distance from operator's hip axis to cg of lower extremities (below hip axis), Z_L , is minimum practical value.
- (8) Operator support location was not shown to be significant; e.g., difference between shoulder or waist attachment.

A. DAMPING ANALYSIS

Figure 13 shows the simplified physical model that was to be analyzed. Assuming θ and δ_c small then the equations of motion are:

$$T = W \text{ or } \ddot{Y}_{cg} = 0, \text{ since } \cos(\theta + \delta_c) \approx 1 \quad (1)$$

$$\frac{W}{g} \ddot{X}_{cg} = T \sin(\theta + \delta_c) \approx T(\theta + \delta_c) = W(\theta + \delta_c) \quad (2)$$

$$\text{Where } I \ddot{\theta} = L_c T \sin \delta_c \approx L_c W \delta_c \quad (3)$$

W = is the weight of the man and his associated equipment (lb)

T = combined thrust of the lifting rockets (lb)

θ = the angular deflection of the body from the vertical (rad) or some desired reference orientation

δ_c = the angular deflection of the thrust vector from the body axis (rad)

I = moment of inertia of the body (slug ft²)

\ddot{X}_{cg} = acceleration of the system cg in the X direction

L_c = distance between the system cg and the thrust vector swivel point.

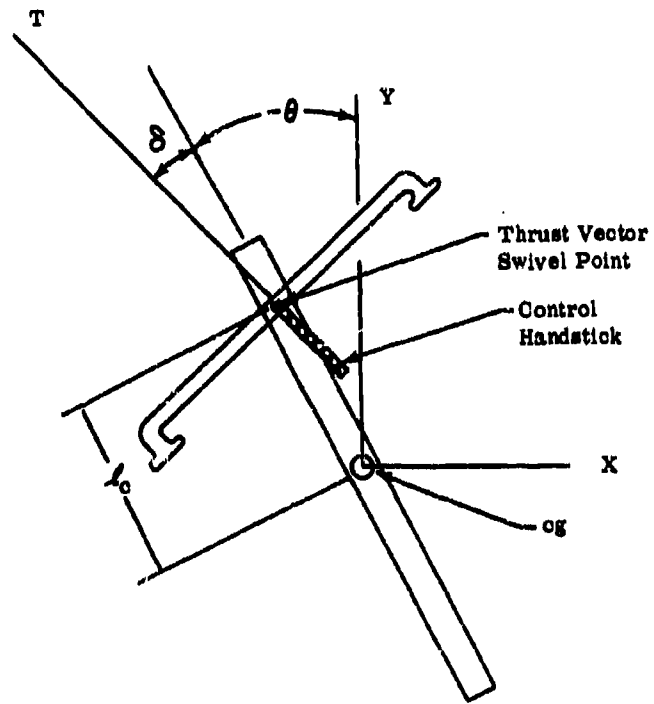


Figure 13. Simplified Rigid Body Model for Damping Analysis

Since it would be very difficult to incorporate a pilot transfer function into the analysis, it was assumed that the pilot's commanded control deflection is proportional to axis attitude error. i.e. $\delta_c = -K\theta$

Equations 2 and 3 then become

$$\dot{x}_{cg} - g\theta(1-K) = 0 \quad (4)$$

$$I\ddot{\theta} + \mathcal{L}_c WK\theta = 0 \quad (5)$$

Applying Laplace transformation to equations 4 and 5 and writing them in matrix form

$$\begin{bmatrix} s^2 & g(K-1) \\ I_s^2 + \mathcal{L}_c WK & 0 \end{bmatrix} \begin{bmatrix} x_{cg} \\ \theta \end{bmatrix} = \begin{bmatrix} 0 \\ 0 \end{bmatrix} \quad (6)$$

The characteristic equation of the system is then:

$$\frac{s^2}{\mathcal{L}_c WK/I} + 1 = 0$$

The transient response is therefore an undamped sinusoid with natural frequency.

$$\omega = \sqrt{\frac{\mathcal{L}_c I.W}{I}} \quad (7)$$

If the system is assumed to have damping, for example if $\delta = \delta_c + \tau \dot{\delta}_c$ and $\delta_c = -K\theta$ (the means whereby such damping can be incorporated into the system is discussed in more detail in a later section) then the equations of motion (2 and 3) become

$$\dot{x}_{cg} - g(K-1 + \tau Ks)\theta = 0 \quad (8)$$

$$\ddot{\theta} + \frac{\mathcal{L}_c KW}{I} (1 + \tau s)\theta = 0 \quad (9)$$

where $\tau =$ a proportional damping gain

The characteristic equation for the system can be written

$$\frac{s^2}{\mathcal{L}_c WK/I} + \frac{\tau s}{1} + 1 = 0$$

with natural frequency

$$\omega = \sqrt{\frac{l_0 W K}{I}}$$

Note: This is the same expression as shown on page when $K_1 = \infty$

and with damping

$$\zeta = \frac{\tau}{2}$$

$$\frac{l_0 W K}{I} = \frac{\tau \omega}{2}$$

It is apparent, therefore, that by properly adjusting τ any desired damping is attainable.

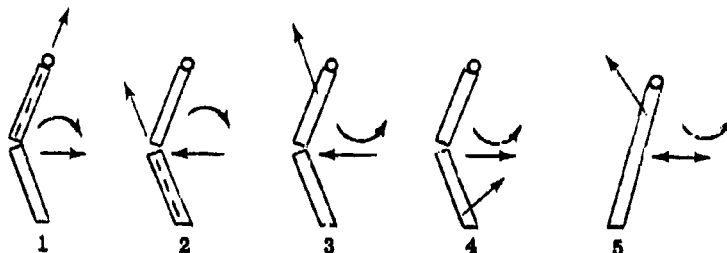
The scheme for obtaining system damping is discussed under three general categories; namely, manual, semimanual, and automatic. Each, of course, requiring successively less attention from the pilot or operator. Before discussing each category separately, some general discussion is in order.

With regard to the manual and semimanual schemes, it is important that the natural frequency of the system be sufficiently low as to be compatible with human response capabilities. There is, however, a practical lower limit on the system natural frequency. In the first place, a very low frequency system is inherently a low loop gain system; hence, the operator will have very limited capability in dealing with gusts or other disturbances since he will have difficulty detecting angular error rate because of the long observation time required. As a result, he will have difficulty damping the motion. This objection does not occur for the semimanual system since the operator need only detect attitude error.

For the completely automatic system, the natural frequency of the system can be much higher and in fact, the natural frequency should be higher than the desired maneuvering frequency so that the automatic damping system does not affect the maneuvering capability. However, the natural frequency for these two categories of damping should not be so high that the human operator has difficulty applying the necessary control moments. Consideration should also be given to the means whereby the operator applies control moments. For example, he will be capable of relatively rapid control moment response if all he has to control is an essentially inertialess control stick or lever. On the other hand, if he is required to bend his body at the middle (cg control) in order to apply control moments, then his response will be considerably slower. In the case of the manual control schemes, the operator is required to detect angular error rates and apply corrective control moments.

In a manual damping system the operator acts as the attitude error and error rate detector, i.e., as the computer, and as the control actuator. In general, control moments can be applied by controlling the relative positions of the system cg or the resultant thrust vector, or both. This can be accomplished by any of the following means or by combinations; (1) rotating the resultant thrust vector about some swivel point, (2) translating the thrust vector laterally, (3) shifting the cg (e.g., bending the body).

Figure 14. sketches 1 through 5 show several possible control schemes.



In sketch 1, the thrust vector is fixed to the upper torso and is directed along the axis of the torso. This arrangement is equivalent to the present experimental rig when the handles and shoulders are held fixed. Attitude errors are corrected by deflecting the legs outward. Damping moments are generated if the legs are deflected in the direction the body is swinging.

Sketch 2 shows the thrust vector fixed to and directed along the legs. Here control and damping moments are obtained by deflecting the legs as described for sketch 1.

Sketch 3 shows the thrust vector pivoted at a point on the upper part of the torso but controlled by the leg deflections as shown in the sketch so that the deflection of the thrust vector more than compensates for the resultant cg shift. For this arrangement attitude errors are corrected by deflecting the legs inward and damping moments are generated if the legs are deflected in a direction opposite to the direction the body is swinging.

Sketch 4 shows the thrust vector pivoted at a point on the lower part of the legs but controlled by the bending as shown in the sketch. Here control and damping moments are generated in the same manner as described for sketch 3.

Sketch 5 shows the arrangement analyzed in the previous section. Here the thrust vector is pivoted on the body axis either above or below the system cg. When pivoted above the cg, the thrust vector is deflected toward the normal to correct attitude error. Damping is obtained by deflecting the thrust vector so as to generate a moment opposing the angular velocity of the body. When pivoted below the cg, the senses of these deflections are of course reversed.

It is interesting to note that all schemes using body bending fall into two categories when classified according to the direction the legs must be deflected in order to generate error correcting and damping moments. It is questionable which direction

of body bending to correct error is closer to the natural instinctive reaction of the human. One of them is used in the present experimental rig. The second, where the feet must be deflected underneath the body to correct errors, seems to be more natural (reaction such as the NACA Flying Platform). A possible arrangement is shown in Figure 15 where the thrust vector is oriented along a line extended between a point above the cg of the torso to a point below the cg of the legs.

The thrust vector control scheme which is recommended is that shown in sketch 5 of Figure 14 with a free swiveling thrust vector and with a low natural frequency.

In the semimanual system the operator is relieved of the task of detecting angular error rate and combining the proper amount of error rate control with attitude control deflection. He need only sense his attitude error and move a control stick accordingly.

Based on the motions of his control stick his attitude error rate is computed and the resultant thrust vector deflection is made up of two parts, one proportional to attitude error rate. This scheme can be implemented with a spring dashpot system shown in principle in Figure 16. Because of the simplicity of the task that the operator had to perform there was considerable optimism that the system would perform satisfactorily.

The feeling was that should this system fail to give satisfactory results then completely automatic systems comparable to aircraft augmentation systems would be considered. Such systems in general, involve rate sensors (rate gyros), amplifiers, and control actuators. A system incorporating all of these components is probably too complex and cumbersome for the application considered here. However, a possible simple system is one which takes advantage of the incoming propellant flow to spin a rate gyro. The upstream side of the injector plate could be quartered by baffles with its spin axis parallel to the flow. Gyro displacements (due rates of body rotation) could deflect the incoming propellant such that one segment (or quarter) receives a higher mass flow. The baffles or tubes would be rifled 90° because of the 90° precession of the gyro. The combustion chamber would also be quartered by baffles extending to the exit of the nozzle. Fixed jetavators would be located at the exit. Body rates would cause the appropriate segment of the combustion chamber to receive higher mass flows and higher pressures. These higher pressures would act on the jetavators to produce a lateral force to oppose the body motion. The entire system may, in the final analysis, be quite simple. Some of the principles of such a system are sketched in Figure 17. Simplified equations of motion for the existing rig, if uncontrolled, are presented in Appendix A.

After a considerable amount of testing on the nitrogen rig, a detailed design of the SRLD began to emerge. A preliminary dynamic system analysis was performed on the design concept to examine the inherent stability aspects of the man-machine combination and to establish the control requirements for various SRLD configurations.

**Operator Acts as Attitude Sensor and Exerts
Control by Bending (Based upon Instinctive Reaction,**

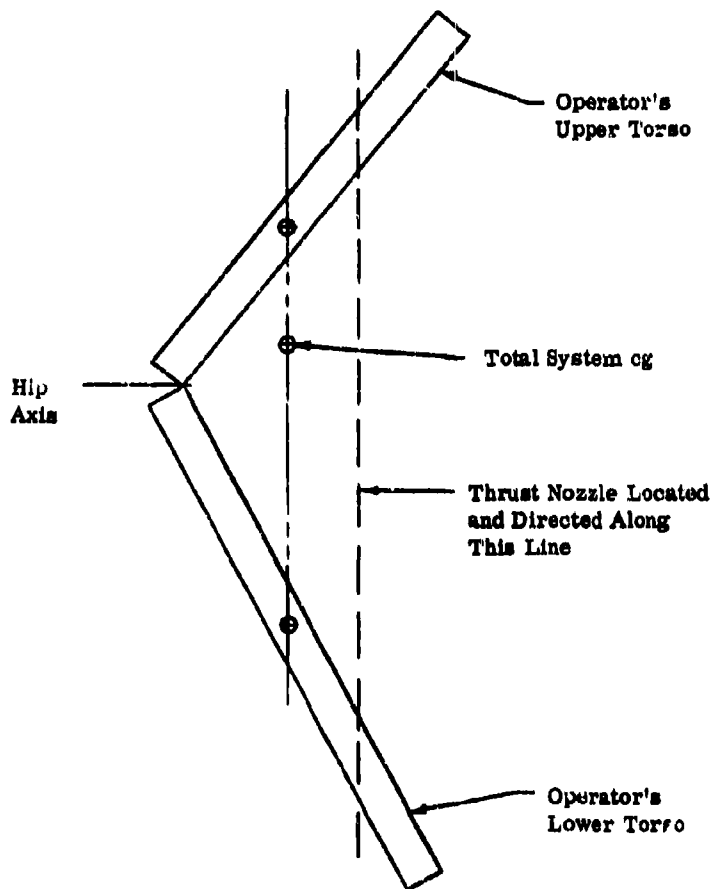


Figure 15. Manual Control and Damping by Natural Reaction

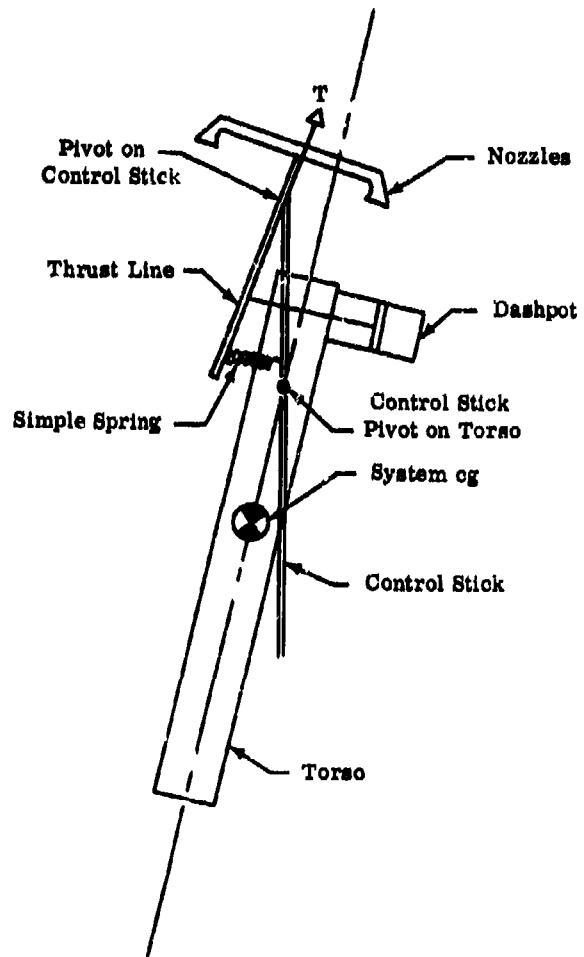


Figure 16. Semimanual Damping

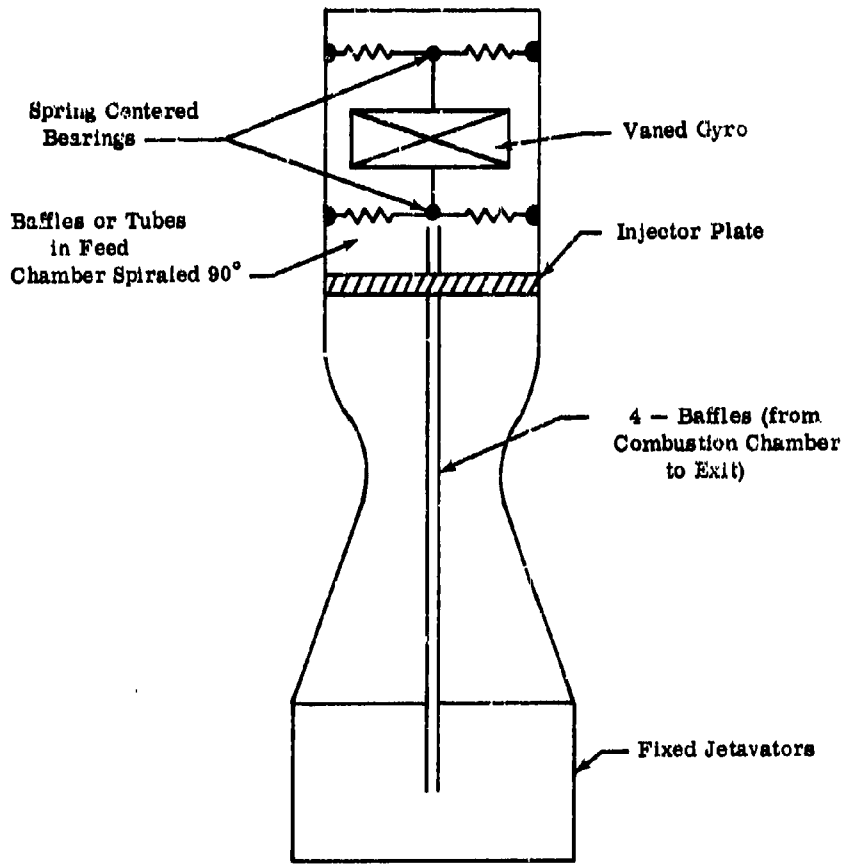


Figure 17. Automatic Damping System

In this report, only the results of a preliminary analysis of the backpack type configuration shown in Figure 18 are presented. This initial configuration was chosen for the dynamic analysis because of its portability and compactness. The analysis compares stability characteristics of this system with and without an automatic stability augmentation device, shown in Figure 19. This device actuates the gimbaled rockets, by sensing the angular acceleration of the backpack rocket belt to provide the man-machine combined system with a desired amount of stability. The dynamic effects of various significant design parameters associated with the stability augmentation device were investigated to establish a functional relationship between design parameters and overall system performance.

The analysis which follows is based on small perturbation concepts and linearized theory. Since a free flight SRLD has six degrees of freedom, consideration must eventually be given to controlling all six modes. However, with throttle setting fixed, the sinking distance of the SRLD due to tilting of the rocket thrust vector is of second order of magnitude as compared with horizontal translation and rotary motion. This is due to the fact that the loss in vertical component of the thrust induced by tilting of the SRLD is proportional to the cosine of the tilt angle, whereas horizontal and rotary effects depend on the sine of this angle. Therefore, the equation of motion in the Z direction was neglected in this first order preliminary analysis. It was also assumed that the dynamics in yaw, possibly arising from heading error correction and/or change in heading, are not coupled with pitch and roll. Thus, yaw dynamics can be treated separately. Also, by inspection of the physical system, neither static nor dynamic coupling exists between pitch and roll. In fact, pitch and roll dynamics should resemble each other qualitatively. Theoretically, the solutions obtained by solving the equations of motion in roll should therefore be applicable to the dynamic system in pitch. Actually, flight tests have shown the pitch motion to be more stable than the lateral motion. Therefore, analyses have emphasized the lateral motions.

Now consider the man-machine combined system perturbed in roll attitude from its initial equilibrium condition. The man-machine combination was represented schematically in Figure 20. The equations of motion are:

$$I_1 \ddot{q}_1 - m_1 g l_2 q_1 - K(q_2 - q_1) + m_1 l_2 \ddot{x} = T_R \delta (l_1 + l_2) \quad (10)$$

$$I_2 \ddot{q}_2 + m_2 g l_3 q_2 + K(q_2 - q_1) - m_2 l_3 \ddot{x} = 0 \quad (11)$$

$$m \ddot{x} + m_1 l_2 \ddot{q}_1 - m_2 l_3 \ddot{q}_2 = T_R q_1 + \frac{T_R}{2} \delta \quad (12)$$

Aerodynamic effects are neglected in this preliminary hovering analysis because for this case the estimated induced moment and drag appeared to be negligibly low. The principal difference between hovering and forward flight is that the moments required for pitch during transition and forward flight would be higher than that required during hovering flight.

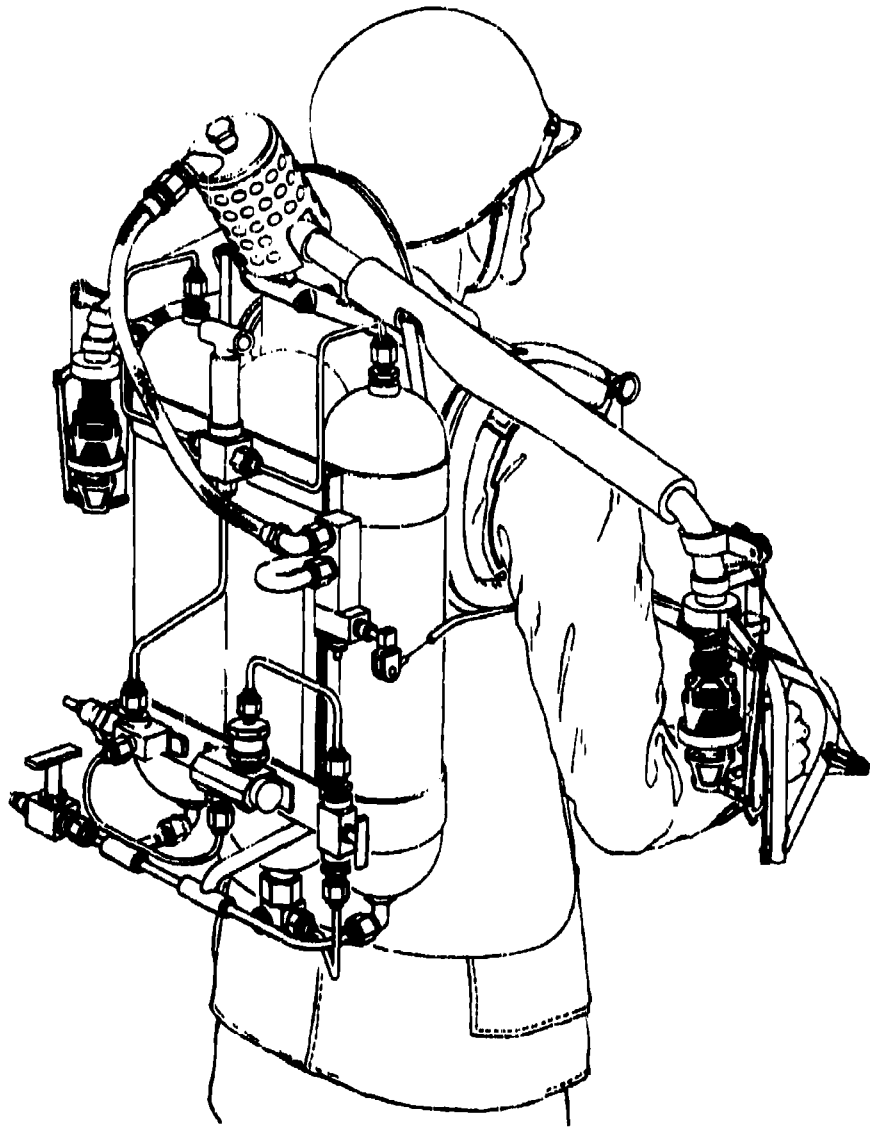


Figure 18. Artist's Concept of Small Rocket Lift Device

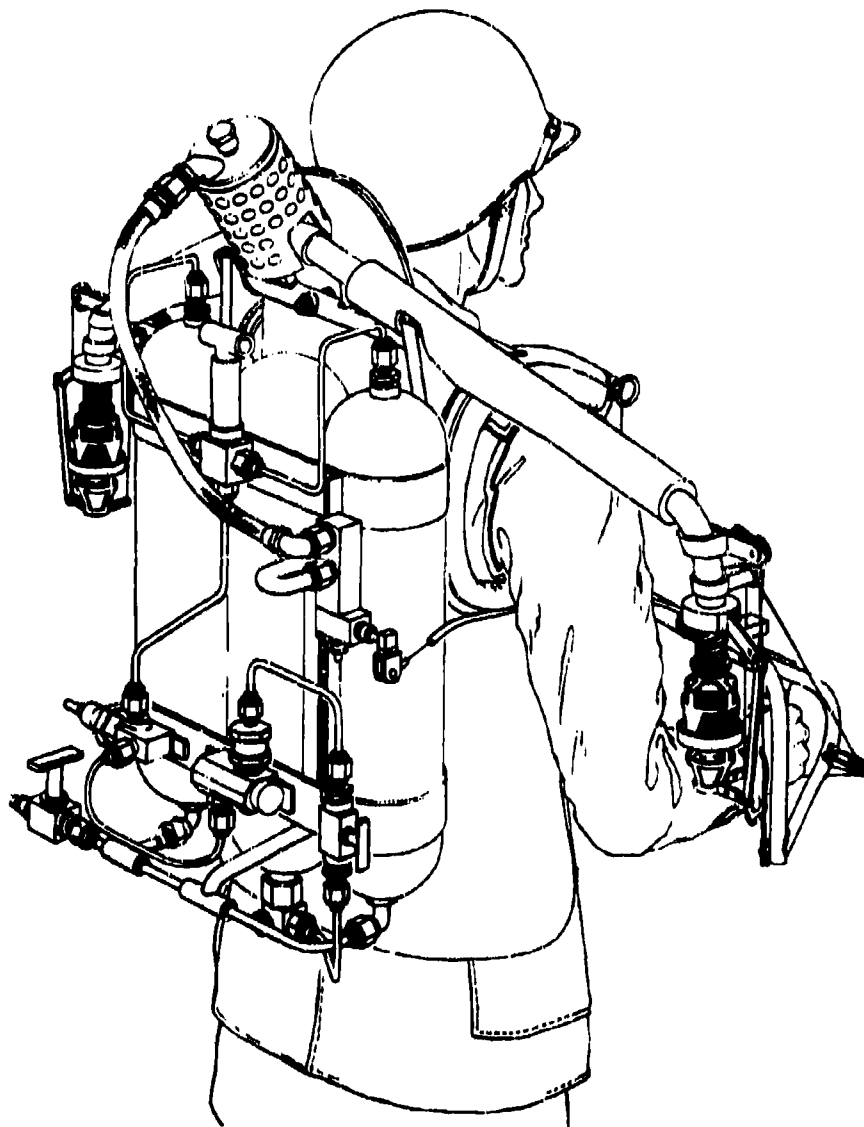


Figure 18. Artist's Concept of Small Rocket Lift Device

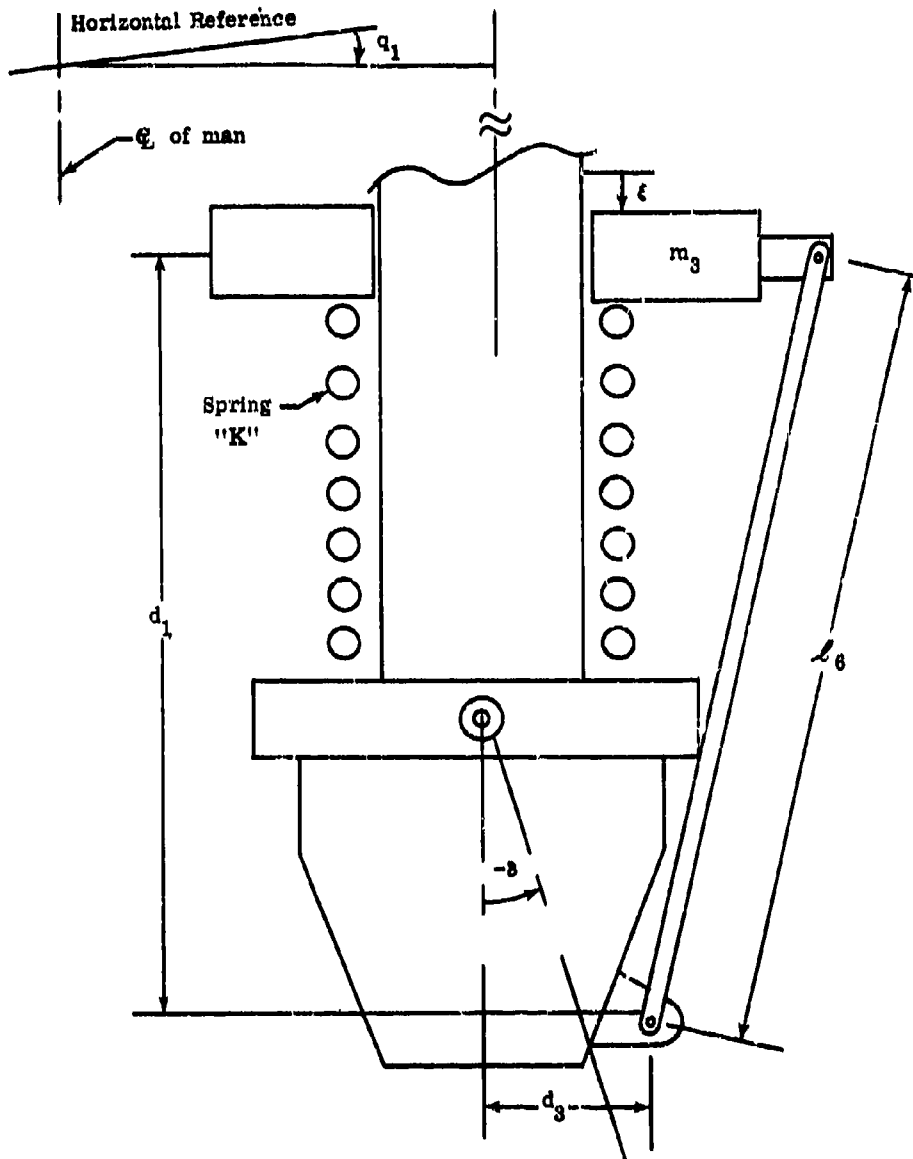


Figure 19. Schematic of Stability Augmentation Device

B. OPEN LOOP ANALYSIS

The open loop system is defined as the man-machine combination without any control. Dynamic behavior of the open loop system should be indicative of system's inherent stability and controllability. The open loop transfer function, relating the roll attitude of the man's upper torso to the deflection angle of the rockets is:

$$\frac{Q_1}{\delta} = K_1 \frac{s^2 + \omega_N^2}{s^2(s^2 + \omega_D^2)} = T \frac{K_2 s^2 + K_3 + K_4 k}{K_5 s^4 + K_6 s^2 + K_1 K s^2} \quad (13)$$

where the pertinent geometry and rotation are shown in Figure 20 and

$$K_1 = \frac{TR}{2} \frac{K_2}{K_5}$$

$$\omega_N^2 = \frac{K_3 + K_4 k}{K_2}$$

$$\omega_D^2 = \frac{K_6 + K_7 k}{K_1}$$

TR = Total thrust of both rockets

$$K_2 = (l_1 + l_2) (m I_2 - m_2^2 l_3) - m_1 l_2 I_2$$

$$K_3 = (l_1 + l_2) m g - m_1 l_2 g m_2 l_3$$

$$K_4 = m (l_1 + l_2 + m_2 + l_3) - m_1 l_2$$

$$K_5 = m I_1 I_2 - m_1^2 l_2^2 I_2 - m_2^2 l_3^2 I_1$$

$$K_6 = m g m_2 I_1 l_3 + m_1 m_2 l_2 l_3 g (m_2 l_3 - m_1 l_2)$$

$$K_7 = m (I_1 + I_2) + 2 m_1 m_2 l_2 l_3 - m_1^2 l_2^2 - m_2^2 l_3^2$$

Both frequencies, ω_N and ω_D , are dependent on the operator's hip "spring" characteristics. These frequencies are shown in Figure 21 as a function of hip stiffness for the full fuel tank configuration. The numerical values of all physical parameters used for the analysis are tabulated in Tables I and II. A root locus plot corresponding to a fuel full configuration with a hip stiffness, K, equal to 100 ft-lb/rad is shown in Figure 19. It indicates that the system is neutrally stable because the open loop poles and zeros are all located on the imaginary axis. In particular, the pair of poles at the origin indicates that once disturbed in roll, the man will continue to roll without restraint. However, flight tests have shown that most men, with very little training, can use kinesthetic control very effectively to stabilize themselves.

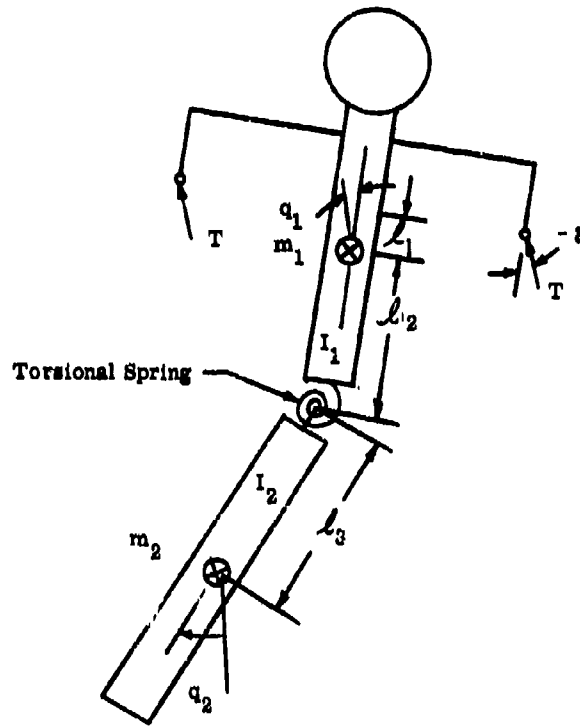


Figure 20. Schematic Representation of Man-Machine Combination

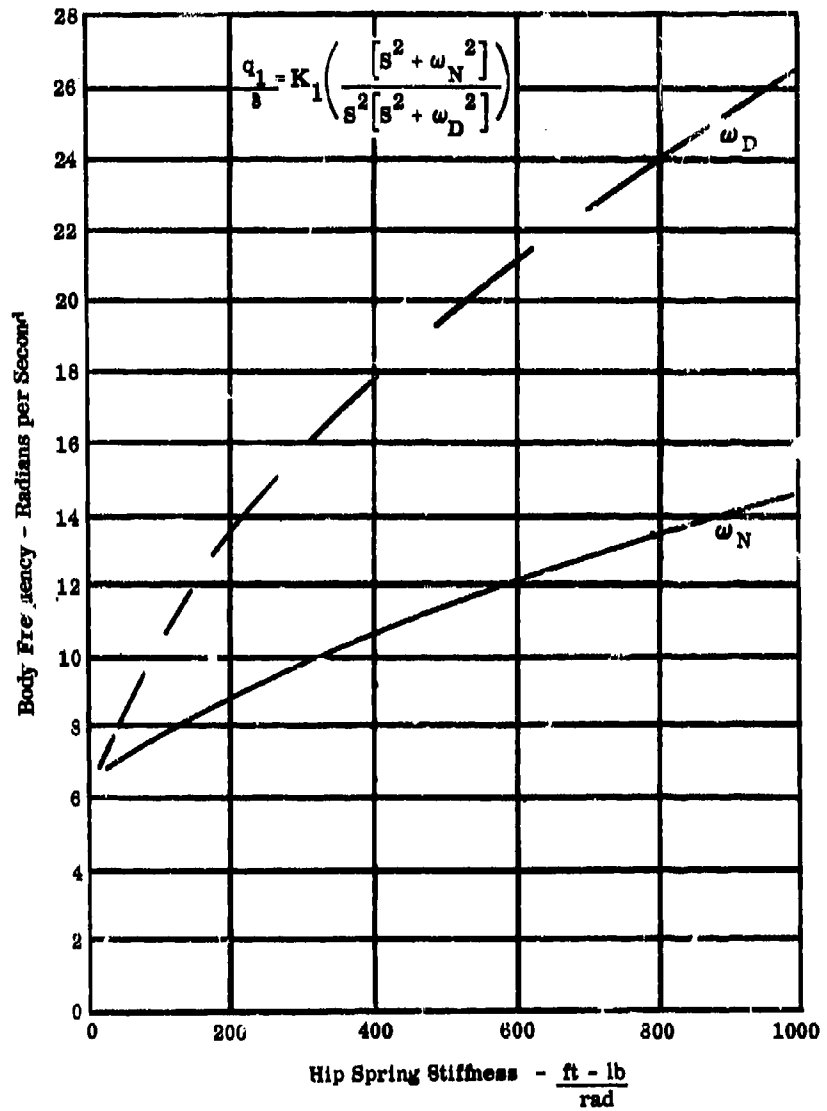


Figure 21. Body Frequency versus Hip Spring Stiffness (Tanks Full)

TABLE I
 WEIGHT ESTIMATE
 SRLD
 MONOPROPELLANT H₂O₂

		<u>Weight</u> <u>(lb)</u>
Tanks		(30.7)
H ₂ O ₂ Tank	(2)	10.0
N ₂ Tank	(1)	16.3
Supports		(4.4)
Straps	(2)	1.1
Vest Support (Plastic)	(1)	3.3
Gas Generator and Catalyst Bed	(1)	6.4
Thrust Nozzles	(2)	3.0
Plumbing and Fittings		3.7
Thrust and Control Tubes		8.1
Valves		5.6
Control Weight	(2)	6.0
Total Dry Weight		(63.5)
Loadable Items		(212.4)
H ₂ O ₂		50.0
N ₂ Gas		2.4
Man		160.0
Total System Weight		(275.9)

TABLE II
NUMERICAL VALUES OF MAN-MACHINE PARAMETERS

Item	Symbol	Units	Full Fuel Conditions	Empty Fuel Conditions
Gross Weight	W_T	lb	258.7	196
Total system center of gravity	cg_T	Inches from top of head	26.3	28.2
Mass of upper body	m_1	slugs	5.69	4.03
Mass of lower body	m_2	slugs	2.06	2.06
Distance from nozzle gimbal point to upper body center of gravity	l_1	ft	0.415	0.474
Distance from upper body cg to total system cg	l_2	ft	0.705	0.910
Distance from lower body cg to total system cg	l_3	ft	1.94	1.73
Hip axis spring constant	K	ft-lb/deg	variable between 50 and 150	
Movement of inertia of upper body about the hip pivot	I_1	slug-ft ²	10.83	7.7
Moment of inertia of lower body about the hip pivot	I_2	slug-ft ²	6.37	6.37

NOTE: The values listed are based on torso data for a Median class man presented in WADC TR 55-159. Weights and cg data of the present Bell Aerosystems ERLD flight test device are included.

C. CLOSED LOOP ANALYSIS

Since the results of the open loop study have shown that the man-machine combination is neutrally stable, a simple automatic stabilizing device might be desirable. This would reduce the amount of attention required and reduce training requirements. Therefore, a mechanically simple yet operational reliable stability augmentation device, was designed and tested. A sketch of the device is shown in Figure 19. The equations of motion, governing the stability augmentation device with mechanical connection to the gimballed rockets are:

$$m_3 l_5 \dot{q}_1 - T_1 \left(\frac{d_1}{l_6} \right) = m_3 \zeta + b_3 \dot{\zeta} + K_8 \zeta \quad (14)$$

$$T_1 \frac{d_1 d_3}{l_6} = I_r \ddot{\delta} + b_r \dot{\delta} + K_r \delta \quad (15)$$

The damping terms have been included for generality although dampers probably will not be used in the final design. The linkage geometry yields a simple relationship as follows:

$$-\zeta = d_3 \delta \quad (16)$$

By solving equations (14), (15), and (16) simultaneously, a feedback transfer function can be obtained as follows:

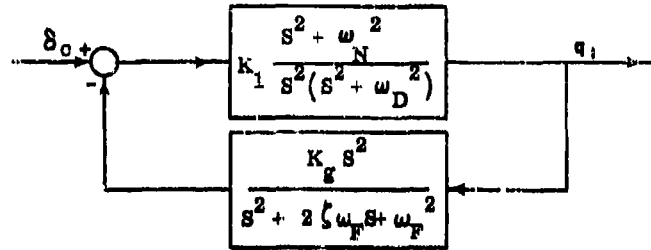
$$\frac{\delta}{q_1} = \frac{-K_9 s^2}{s^2 + 2 \zeta \omega_F s + \omega_F^2} \quad (17)$$

$$\text{where } K_9 = \frac{m_3 l_6}{m_3 d_3 + \frac{I_r}{d_3}}$$

$$= \frac{b_3 d_3 + \frac{b_r}{d_3}}{2 \sqrt{\left(m_3 d_3 + \frac{I_r}{d_3} \right) \left(K_8 d_3 + \frac{K_r}{d_3} \right)}}$$

$$\omega_F = \sqrt{\frac{K_8 d_3 + \frac{K_r}{d_3}}{m_3 d_3 + \frac{I_r}{d_3}}}$$

A functional block diagram of the overall closed loop SRLD with the stability augmentation device will be shown as below.



The two zeros in the feedback transfer function cancel the two poles at the origin in the forward transfer function. However, the closed loop transfer function still contains an s^2 term in its denominator. Therefore, the stability augmentation device does not eliminate the neutral stability in roll. However, preliminary analog computer studies show that the rate of roll resulting from an external disturbance can be greatly reduced by the stability augmentation device. Thus the pilot is relieved of a requirement for fast response to keep the roll angle within bounds.

There is also a theoretical neutral stability of the leg swinging mode. Flight tests have shown that actually this mode is of no concern to most operators even with no damper provided in the control device. This is probably due to the inherent damping of the man, to his nonlinear stiffness characteristics, and his inherent ability to control very lightly damped oscillations. Further analysis and testing is required to determine the optimum system parameters. However, preliminary studies have shown that the oscillatory mode can be given almost any desired degree of stability with judicious design of both gains K_1 and K_2 and the control device damping constant and the roll rate resulting from external disturbances can be significantly reduced by this design. Therefore, it appears feasible to design a system which should be controllable by the most inexperienced personnel.

The root loci of the closed loop for various ω_F and ζ are plotted in Figure 22. Note that stability of SRLD becomes relatively poor if the frequency of the stability augmentation device is comparatively large. This is obvious because a stiff spring between the bob weight and gimbaled rocket virtually eliminates any desired relative motion between them. Conversely a very soft spring produces a system which is susceptible to vertical accelerations and disturbances. Therefore, care must be exercised in designing the mechanical components of the stability augmentation device in order to obtain desirable performance.

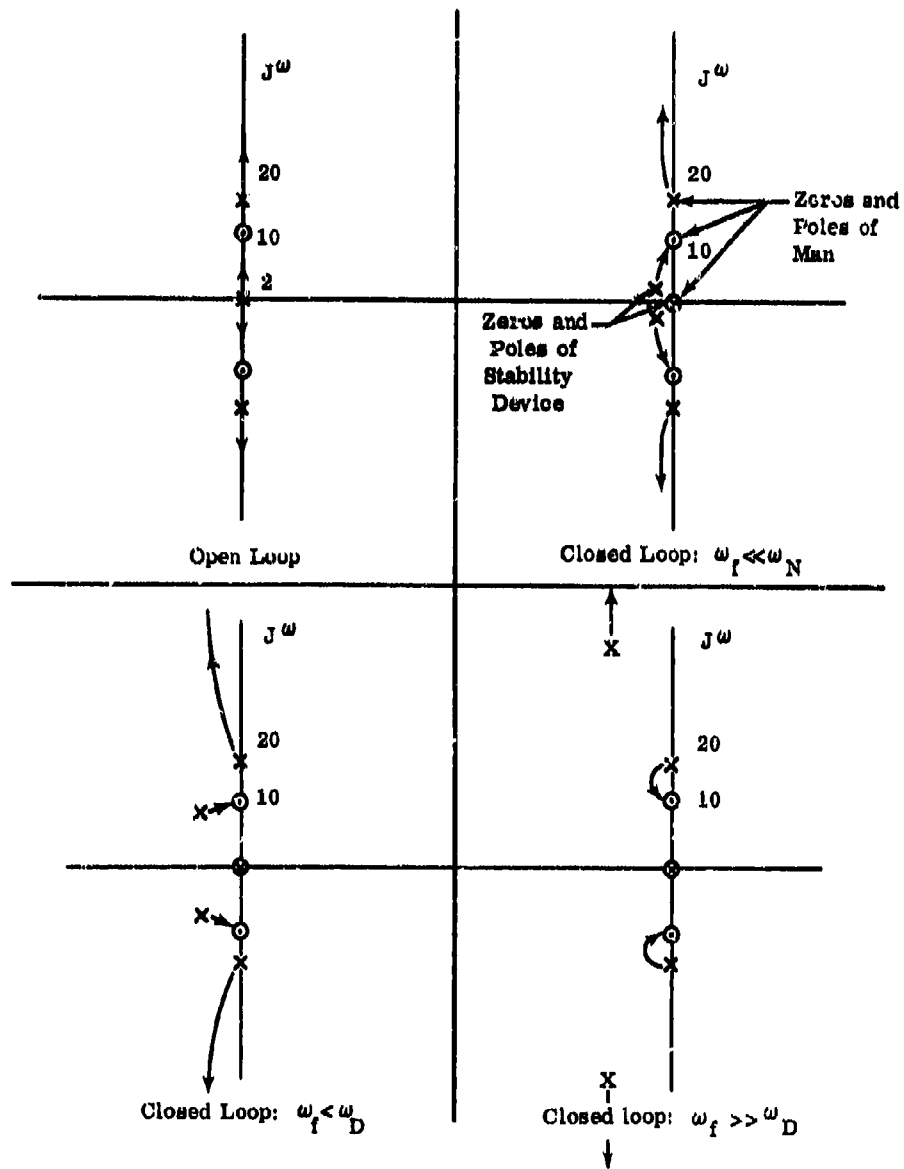


Figure 22. Root Loci

D. ANALOG COMPUTER STUDY OF OPEN AND CLOSED LOOP

The SRLD system with the stability augmentation device was simulated on a Reeves Electronic Computer. The computer diagram is shown in Figure 23. Early results of the REAC studies showed that the effect of the difference of the angular deflections of the upper body (q_1) and lower body (q_2) is negligibly small. Therefore, the man-machine combination was assumed to be a rigid body for the preliminary studies discussed in the following paragraphs. The criteria used for evaluation of system performance are the rate of roll and horizontal velocity resulting from external disturbances.

Figure 24 shows the open loop response of the SRLD to a disturbance force of approximately 25.8 pounds applied 0.899 feet above the cg of the man-machine combination. This is considered to be a very severe disturbance. The resulting rates of roll and translation are $67^\circ/\text{sec}$ and $15 \text{ ft}/\text{sec}$, respectively. The angle of roll, of course, far exceeds the limit of validity of the analysis but the results still serve for qualitative comparisons with other cases. With the stability augmentation device, ($\omega_F = 5 \text{ rad}/\text{sec}$ and $\zeta = 0.5$) in the feedback loop, the rates of roll and translation are reduced to $12^\circ/\text{sec}$ and $10 \text{ ft}/\text{sec}$ as shown in Figure 25. This indicates a significant improvement of the system performance due to the augmentation device. Figures 25, 26, and 27 demonstrate the negligible effects of various dampings used in the stability augmentation device with $\omega_F = 5 \text{ rad}/\text{sec}$. With a realistic damping ratio, ζ , of 0.1, the frequency effects on the rates of roll and translation are shown in Figures 27 and 28. This comparison indicates that lowering the undamped natural frequency of the stability augmentation device results in significant reductions in the rates of roll and translation. Increasing the ratio l_2/d_3 results in a significant decrease of the rates of roll and translation as shown in Figures 25 and 29.

The results discussed above show that the stability augmentation device can be designed to reduce the rates of roll and translation to values which will permit even inexperienced men to exercise kinesiologic or manual control and easily keep the roll angle and distance traveled to very small values. However, the natural frequency of the mass-spring system must be of the order of $10 \text{ rad}/\text{sec}$ (2 cps) or less if the stability augmentation device is to be effective. Such low frequencies imply that the control system will be quite sensitive to vertical accelerations. However, if the rocket gimbal deflections due to vertical accelerations are limited to 15 degrees, the maximum loss of vertical thrust is only about 3 percent of nominal thrust.

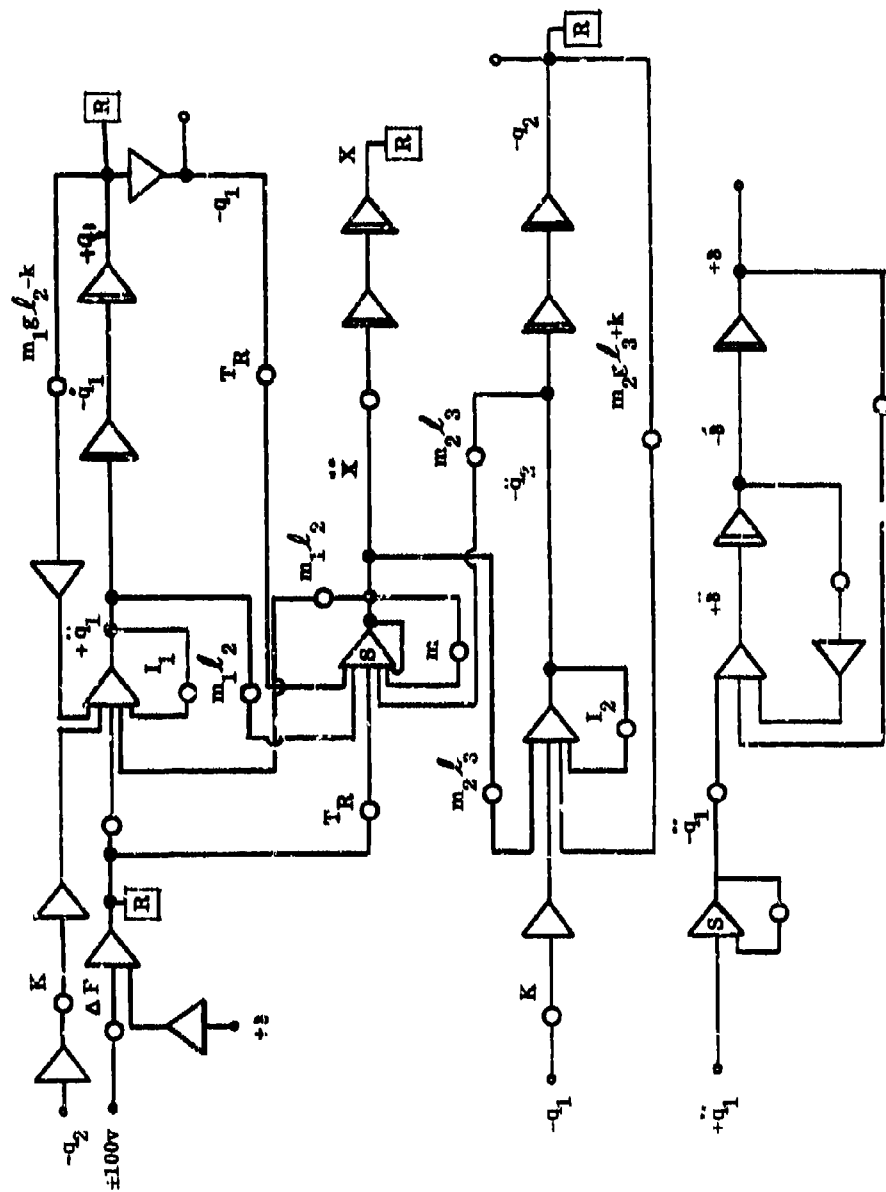


Figure 23. Analog Computer Diagram

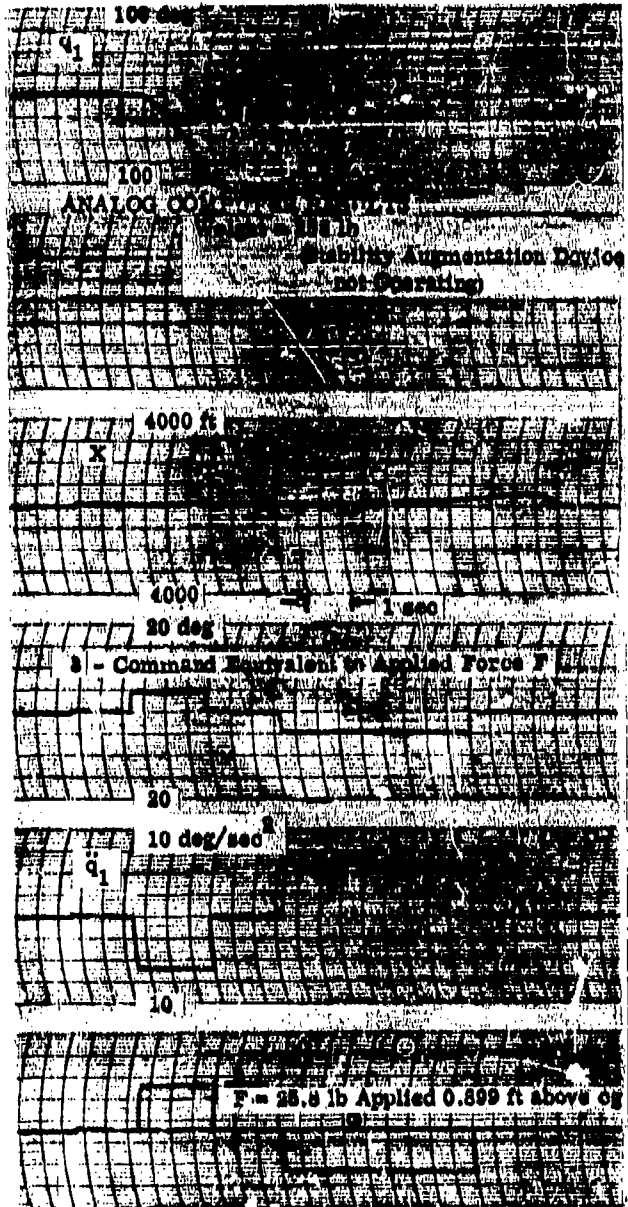


Figure 24. Analog Computer Results

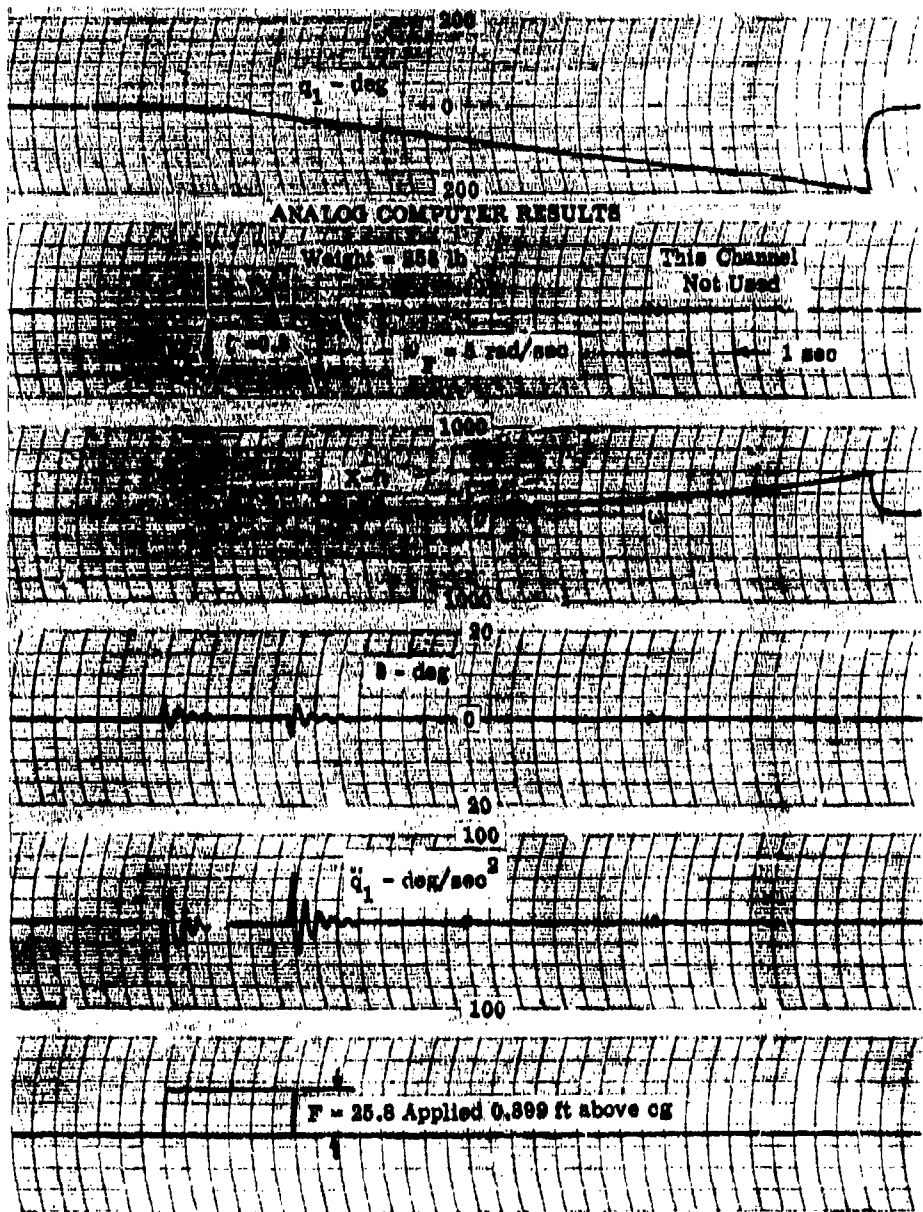


Figure 26. Analog Computer Results

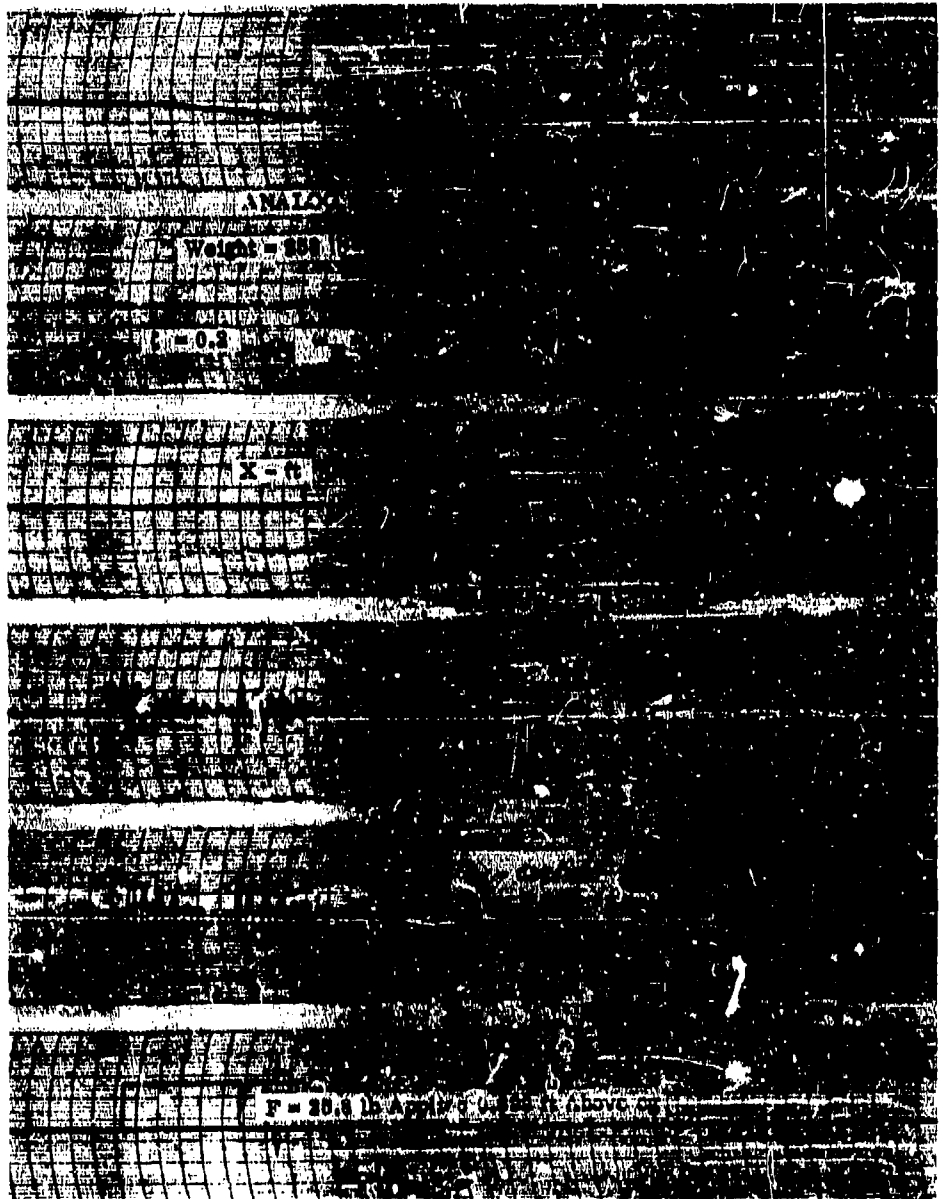


Figure 26. Analog Computer Results

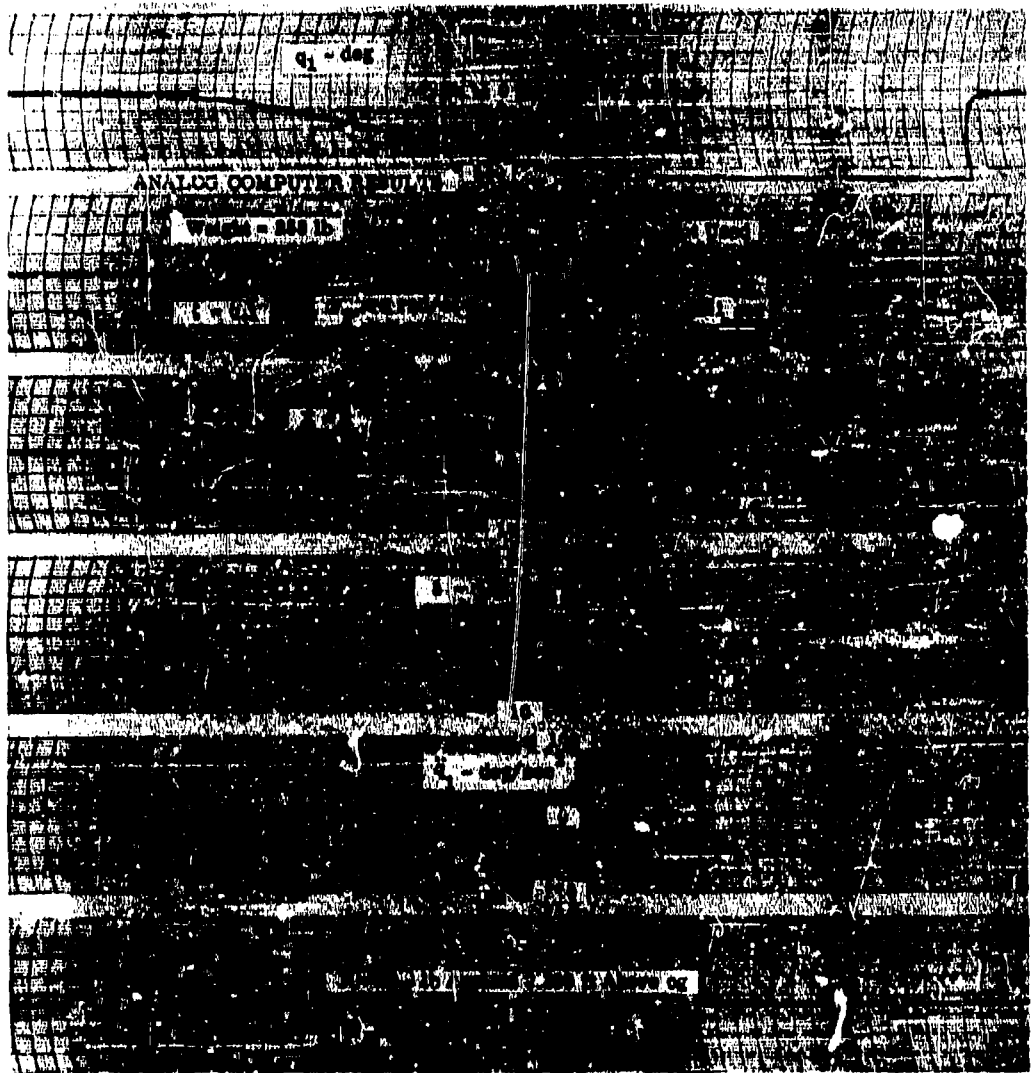


Figure 27. Analog Computer Results

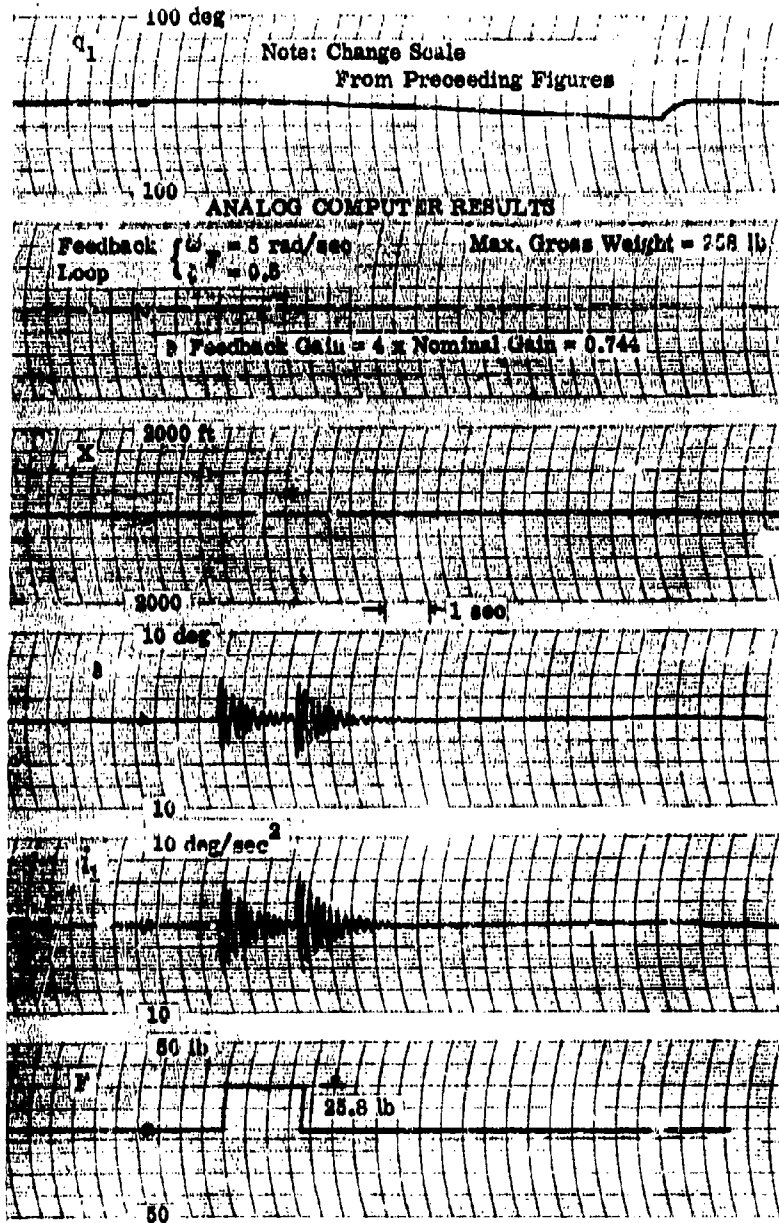


Figure 2'. Analog Computer Results

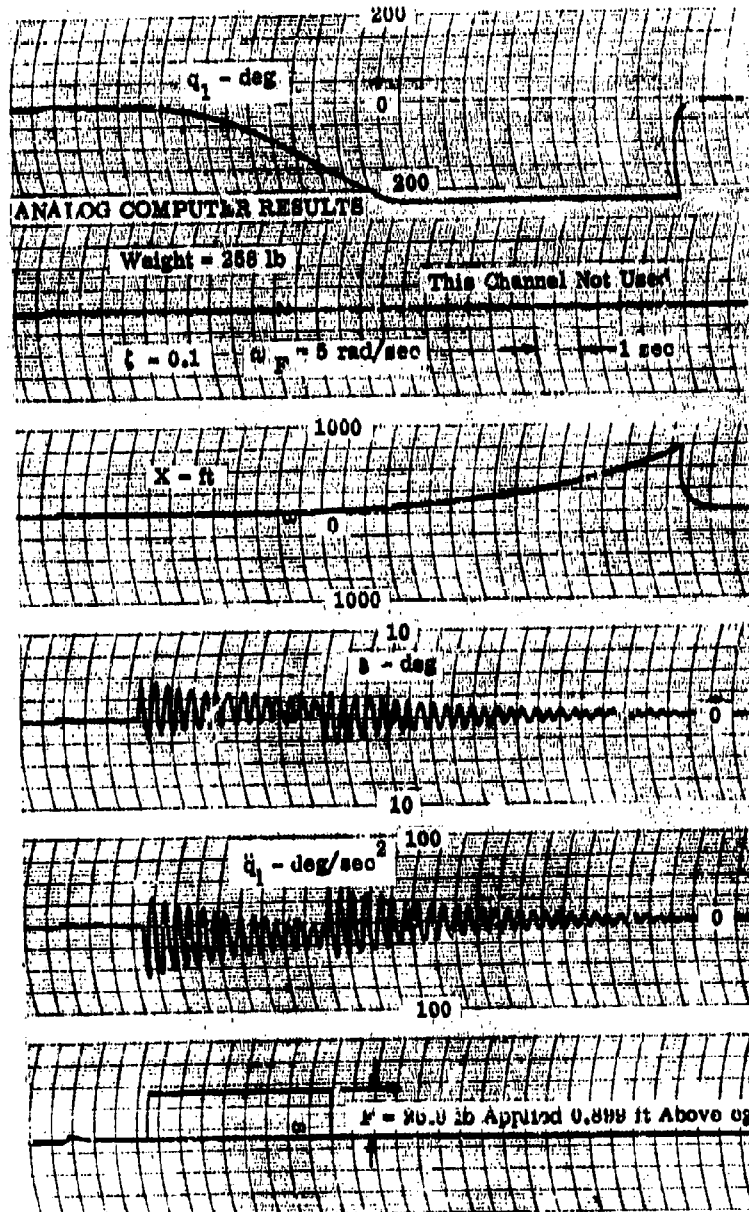


Figure 29. Analog Computer Results

SECTION IV. DEVELOPMENT OF THE ZERO-G BELT

The initial design of the Bell Zero-G Belt was essentially derived from a number of theoretical analyses, related experience with the rocket belt, and the Air Force's experience with the Mark I and Mark II propulsion systems. The objective for building the Bell system was, through flight testing in the C-131, to generate information for developing simple and reliable equipment that would augment the space worker's capability to do extravehicular work.

A major decision had to be made early in the design as to whether or not the system would require automatic stabilization of the man. It was recognized that for the space worker to effectively accomplish his tasks, he must be able to stabilize and control his attitude about three axes and to stabilize and control his spatial position with respect to orbiting objects on which he might be required to perform maintenance functions. However, the means by which this might be accomplished may be fully automatic or involve no automatic equipment at all, as dictated by the nature of the tasks and the basic capabilities of the worker. The following considerations led to a decision to reject the use of automatic stabilization in the first system:

- (1) Experience with the SRLD provided conclusive evidence that under conditions of a one-g environment, a man can manually stabilize his attitude and control his flight path.
- (2) Air Force personnel who at that time had the most extensive experience with the operation of man-propulsion systems under zero gravity, were of the opinion that manual stabilization and control might be feasible.
- (3) Until an adequate propulsion system was made available to evaluate the learning factor and to define the parameters and degree of control and stability required, a final decision for automatic versus manual stabilization and control could not be made.

Figure 30 functionally illustrates the overall concepts and indicates the inter-relationship of human sensing and body dynamics with the control forces and the parameter to be controlled and stabilized. Note the inner loop which can have a stabilizing or destabilizing effect. During the use of the belt in flight tests, learning trends which could produce stability in this loop were to be closely noted. Also, by assessing the operator's capability for controlling position, rate and acceleration in both translation and rotation, it was felt that an optimum combination between a manual and automatic system might be defined. Furthermore, the desirability of an on-off versus a proportional control system might be examined if throttleable thrust could be achieved. Again, it was recognized that there might be limit cycle oscillations inherent in an on-off stabilization system which, when coupled with the flexible

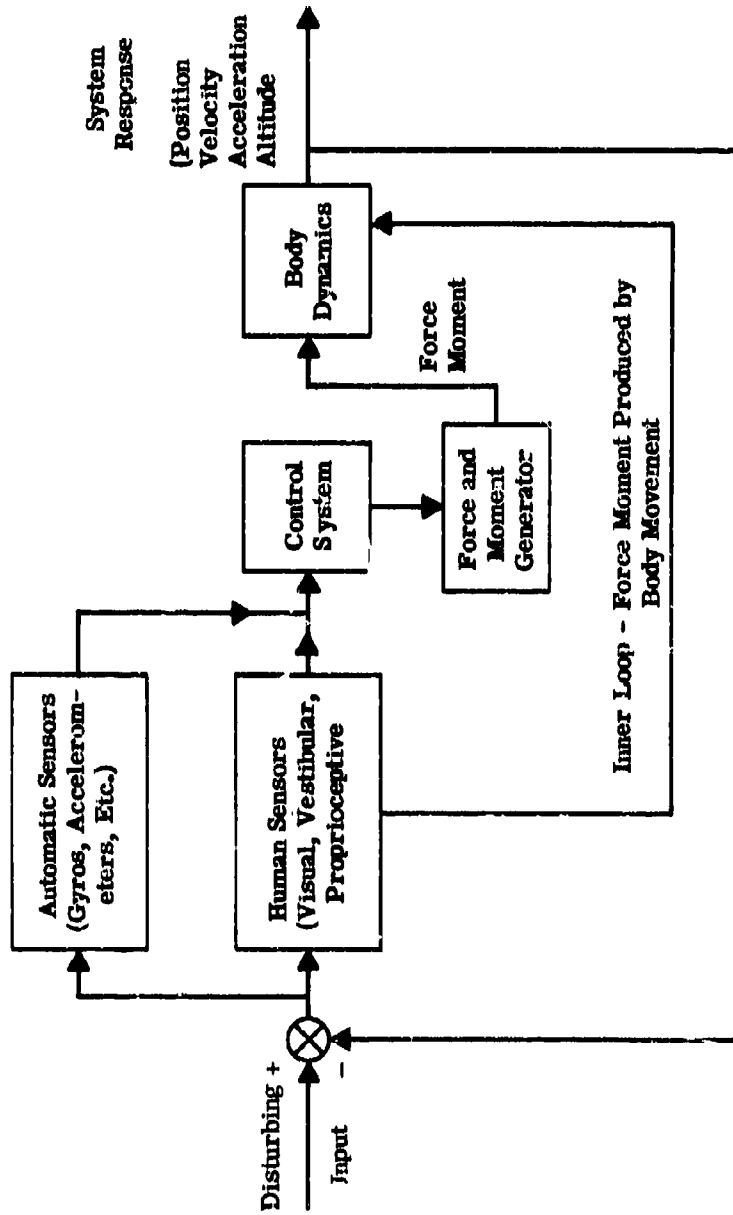


Figure 30. Functional Block Diagram of the Stability and Control System.

response of the worker's body, could induce unacceptable stability. On the other hand, some types of proportional control were considered to be costly in terms of weight, bulk, and reliability.

Prior to the initial work on the zero-g belt, considerable stability and control experience was gained through analytical and analog simulation studies, flight test experience on the SRLD, and evaluation of NASA studies on one-man lift devices. While it is recognized that extrapolation of results and conclusions to the zero-g flight condition is difficult, tests conducted at Bell Aerosystems Company did indicate the feasibility of a manual type control system for the space worker. The tests which investigated the flying qualities of a man in a one-g belt indicated the following relationship to the zero-g flight operation: (1) low values of thrust for angular attitude control are desirable, and because of the zero-g flight condition, they can be selected largely independent of the translational thrust requirements, although some coupling of modes does occur (angular control in this case would be supplied by pure torque couples); and (2) proper selection of thrust levels and control arms could provide satisfactory manual stabilization and control characteristics under hovering or translation control.

The first configuration of the zero-g belt therefore represented a starting point from which succeeding analyses were conducted.

In this system, man is analytically represented by a two-segmented body in which the upper and lower torso are connected by the hip socket effective spring. Figure 31 depicts this model.

The equations of motion in the orbit plane are:

Upper Torso Rotation

$$I_1 \ddot{q}_1 - K(q_2 - q_1) + 57.3 M_1 \ell_1 \dot{X}_B = T_R \ell_R + M_{E_1} \quad (18)$$

Lower Torso Rotation

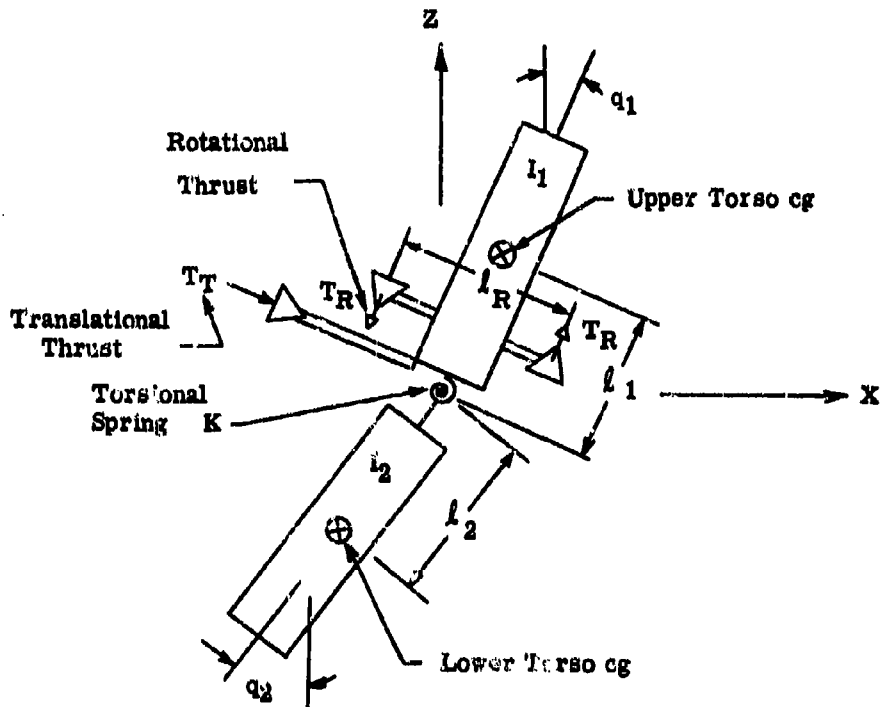
$$I_2 \ddot{q}_2 + K(q_2 - q_1) - 57.3 M_2 \ell_2 \dot{X}_B = M_{E_2} \quad (19)$$

Complete Body Longitudinal Translation

$$57.3 M \dot{X}_B + M_1 \ell_2 \dot{q}_1 - M_2 \ell_3 \dot{q}_2 = F_T + F_E \quad (20)$$

$$\text{and } \dot{X} \text{ (along orbit path)} = \dot{X}_B \cos q_1$$

Vertical Translation (In the Orbital Plane)



Definition of Nomenclature:

- | | | |
|-------|---|------------------------------------|
| q_1 | = Angular displacement of upper body from the vertical | |
| q_2 | = Angular displacement of lower body from the vertical | |
| I_1 | = Moment of Inertia of upper body about hip pivot | |
| I_2 | = Moment of Inertia of lower body about hip pivot | |
| l_1 | = Distance between upper body Center of Gravity and hip pivot | |
| l_2 | = Distance between lower body Center of Gravity and hip pivot | |
| l_R | = Reaction jets moment arm | |
| T_R | = Thrust level of reaction jets used for rotation | |
| T_T | = Thrust level of reaction jets used for translation | |
| K | = Effective torsional spring constant of hip pivot | |
| M_1 | = Mass of upper body | Z = Vertical displacement |
| M_2 | = Mass of lower body | X = Longitudinal displacement |
| M | = Total mass of body | λ = Gravitational constant |
| W | = Total weight of body | |

Figure 31. Two-Segment Body Model

$$MZ = \frac{M(V_c + \Delta V)^3}{R_c + Z} - Mg$$

Where

V_c = circular orbital velocity

R_c = circular orbital altitude

$$\text{or } \ddot{Z} = \frac{V_c^2 + 2V_c \Delta V + \Delta V^2 - g}{R_c + Z}$$

but since

$$Z \ll R_c, \Delta V \ll 2V_c \Delta V, \frac{V_c^2}{R_c} = g$$

$$\text{and } V_c = \sqrt{\frac{\lambda}{R_c}}$$

then the simplified equation becomes.

$$\ddot{Z} = \frac{2\sqrt{\lambda}}{R_c^{3/2}} \Delta V \quad (21)$$

at 300 n.mi. orbit

$$\ddot{Z} \approx 1 (10^{-3}) \Delta V$$

which indicates that vertical displacement from the work area can be neglected for ΔV 's < 10ft/sec and translation times < 10 seconds. These equations assume rectilinear motion in orbit.

The moments $M_{E_1}(t)$ and $M_{E_2}(t)$ and force $F_E(t)$ are applied moments and forces due to work tasks or body component muscular accelerations. (It was assumed that these could be more accurately defined and described during future studies on an air bearing platform and by one-g and zero-g belt flight tests.) The equations of motion in a plane transverse to the orbit plane can be written in a similar fashion by modifying equation (21). It has been determined from previous analyses that such a system is neutrally stable. Stabilization and control are manually provided through operation of the reaction thrust units T_R and F_T . However, it was recognized that evaluations and analysis of the flight characteristics of this control system could best be accomplished by analog simulation. Future work was planned utilizing the same

techniques which were successful in determining the "flying qualities" of the one-g belt; that is, using a physical hand controller (similar to the present zero-g belt design) as the pilot's input to the analog computer in a one-plane simulation setup based upon the equations described above. The human operator or pilot would then provide control inputs based on visual observation of this position and motion on an oscilloscope display. The oscilloscope display would show: (1) angular attitude of the upper body; and (2) longitudinal and vertical translation in the orbital plane. This is illustrated in Figure 32. Figure 33 shows the analog simulator in operation as it was used in the SRLD program.

A study of this type would simulate the longitudinal (pitch and forward translation) and vertical degrees of freedom, and then be modified as required to include stability augmentation system dynamics. Specific tasks could be assigned, such as rotating and translating to a given position on the scope display. During the transit, external disturbances and/or kinesthetic motions could be introduced as time history moment and force inputs.

The variable design quantities or parameters that were envisioned for investigation are:

- (1) Translational thrust levels and thrust locations (a position slightly above the cg may be advantageous in counteracting vertical motion due to orbital mechanics).
- (2) Angular torque levels.
- (3) Fixed versus rotating thrust units.
- (4) Hand controller design characteristics.

In evaluating the handling or performance characteristics of the manual control system for each of the design parameters, a systematic rating system could be established. Unfortunately, this study was not accomplished due to lack of funding. It is described as a relevant methodology for the development of future systems.

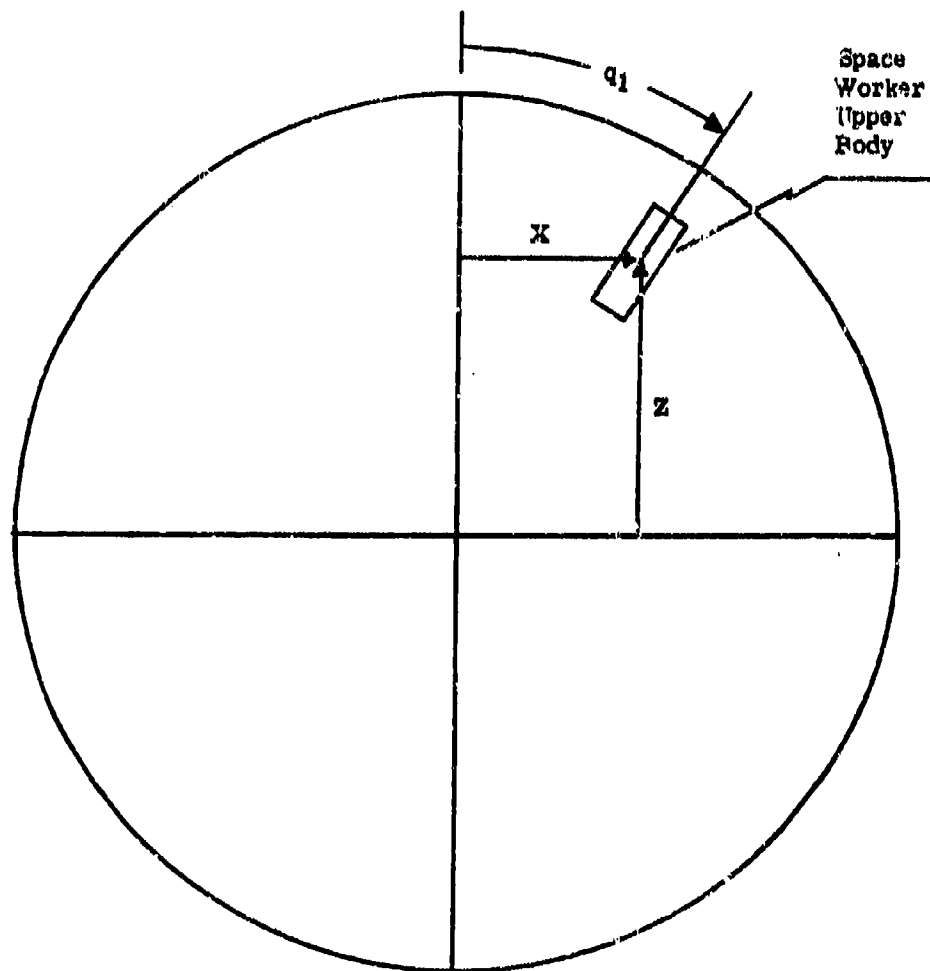


Figure 32. Oscilloscope Display Schematic



Figure 33. Analog Flight Simulator

SECTION V. HARDWARE DEVELOPMENT PROGRAM

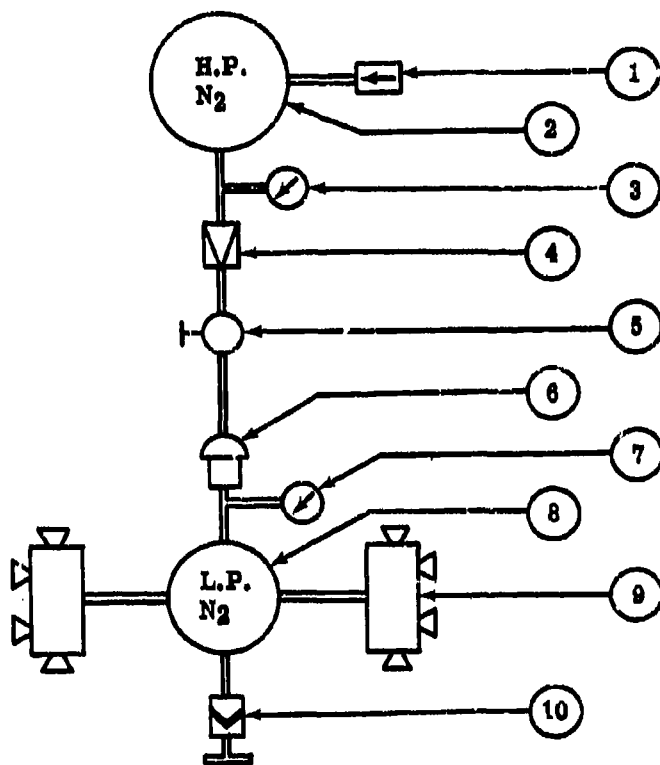
Construction of the Bell Zero-G Belt was started in December 1960. Specific design details were formulated with respect to the mission for which the unit was conceived; e.g., as a research tool to study the capability of a man to position, stabilize and translate his body in a zero-gravity environment. The rationale for the design approach in general was discussed in the previous section and the specific design requirements to permit flight testing of the unit were discussed in Section II under Concept Development.

A schematic of the original system is presented in Figure 34. The function of the system is quite simple. Super dry nitrogen is stored in the high pressure tube bundles. Upon activation of a thrust controller, the N_2 gas flows from the high pressure tubes through a gauge and a filter to the regulator. The regulator takes the high pressure gas and converts it to a low pressure supply in the low pressure tubes. Low pressure N_2 is thus stored until the throttle valve is opened when it escapes through the nozzles to produce thrust.

Of all the components depicted in the schematic, only the thrust and directional control unit ⁽⁹⁾ required pre-design testing. All of the other items had been tested and used in previous Bell programs. A sample ten-pound thrust orifice was constructed and tested in Bell's Propulsion Laboratory.

The Zero-G Belt consists of high pressure tube bundles attached to a snugly fitting fiber corset worn on the middle of the torso. Two thrust controller units are placed on the belt at the cg level of the body, one on each side. Each unit contains a manifold block into which are installed eight gas orifices with integral shutoff valves. The orifices, or thrust valves are controlled as desired by the operator to propel himself in any direction or axis of rotation. To effect this control, the operator simply pushes, pulls, lifts, depresses, or rotates the hand controllers in the direction he desires to translate or rotate. For example, pushing down on the controllers opens up the two top thrusters on each manifold block, forcing the operator in downward direction. Pushing forward on the controllers opens the rear thrusters, moving the operator forward. For rotating about the vertical axis, forward pressure is used on one controller and rearward pressure on the other. Thusly, by proper use of the controllers, motion in any of the six translational directions, six rotational directions, or combinations of rotation and translation can be achieved.

The controls are self-centering and require a force of six pounds for actuation. Control motion is approximately 1/4 inch and the valves are either half open or full closed. The maximum thrust of the assembled unit at the completion of the development program, produced at sea level pressure, was measured at 16.35 pounds.



Legends:

1. Schrader Fill Valve
2. H.P. Tube Bundle
3. H.P. Gage
4. Filter
5. Manual Shutoff Valve
6. Regulator
7. L.P. Gage
8. L.P. Tube Bundle
9. Directional Control Valve (2)
10. Burst Disc

Figure 34. Zero-G Belt Schematic

Thrust at this level can be continuously maintained for 11 seconds. Although this is a relatively short duration, thrusts of this level used in pulses were assumed to be minimally sufficient for maneuvering during the relatively short periods of weightlessness that can be produced in a C-131 aircraft.

Initial tests on the valve design showed less thrust than was anticipated from theoretical calculation. A small amount of rework on the assembly to increase chamber pressure was accomplished. Retest was completed January 5, 1961, with the following results:

	<u>Chamber Pressure</u>	<u>Thrust</u>
1st Test	165 psig	6.25 lb
2nd Test	185 psig	7.5 lb

The rework raised the chamber pressure 20 psig and the thrust 1.25 pounds.

Theoretical calculations indicate that 10.3 pounds of vacuum thrust and 7.7 pounds of thrust at sea level should result with a 165 psig chamber pressure. Sea level thrust should be 9.5 pounds at 185 psig chamber pressure. Results of this test were sufficient to proceed with the design of the thrust controllers.

These units consist of manifold blocks into which are installed gas orifices with integral shutoff valves. These orifices are suitably positioned to produce thrust essentially through and about the cg. Figures 35 and 36 respectively show a top and side view of the unit.

Construction started on the tube bundle assembly in early January 1961. The high pressure tube bundles for storage of high pressure into gas were formed from 1-1/4 in. x 0.035 in. 4130 steel tube. These tube bundles were made in lefts and rights and curved to fit the torso. The assemblies were terminated at the rear to a set of manifold plugs. The inside rows of tubes (8 in all) were high pressure. On the outside set of tubes, 5 were high pressure and the lower 3 were low pressure. The left and right tube sections were hinged at the terminating manifolds to allow for easy donning and removal of the assembly. At the front, all tubes were terminated by welding tight fitting plugs into the ends of the tube. All of the plugs were drilled and tapped for either attaching pressure lines, or for inspection and drain provisions. Those holes not used for attachment of fittings and pressure lines were sealed with 1/4-inch Parker Lock O seals. All tubes terminating at the rear manifold were swaged down to a dimension allowing for access during the welding operation. Figures 37 and 38 show the configuration of the tube bundles.

Upon completion of welding and attachment of the hinge, the high pressure tube bundles were heat treated to a 170,000 psi minimum. The low pressure tube bundle assemblies were constructed out of 0.035 Aluminum-Alloy tube and were brought up to the TO condition.

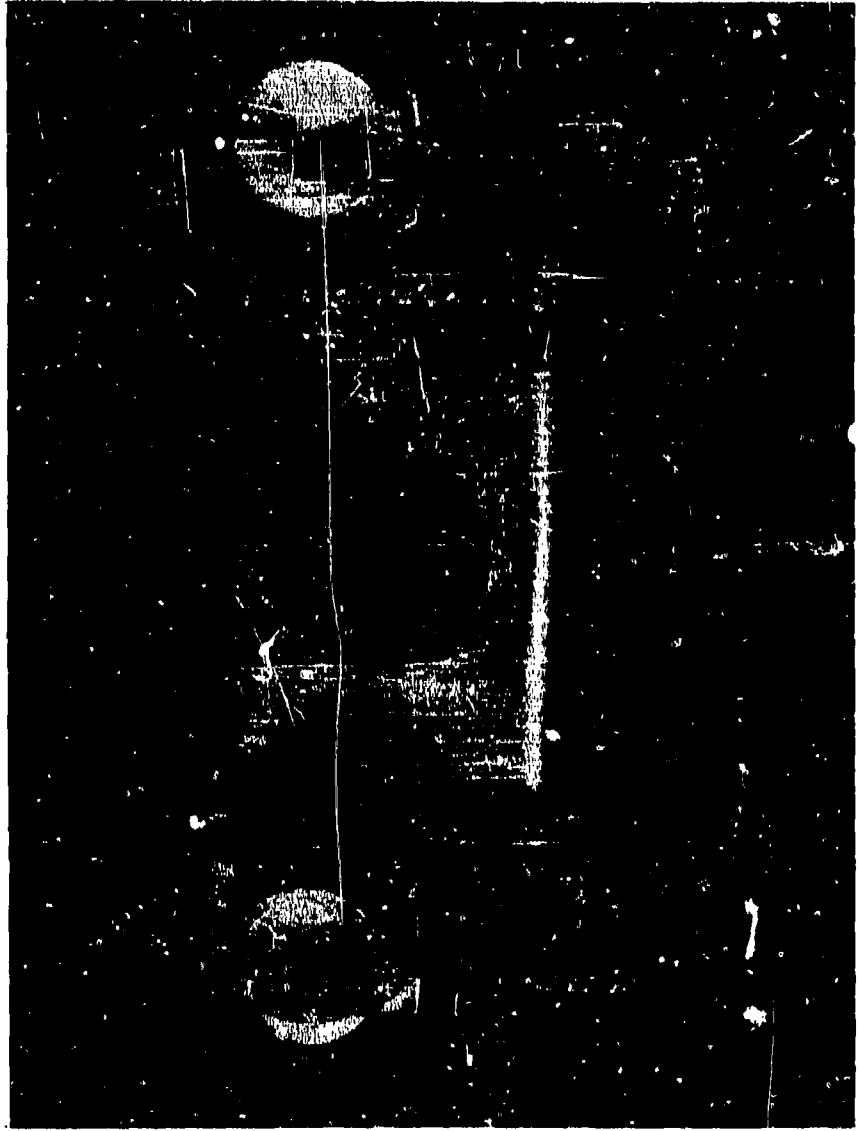


Figure 35. Top View of Thrust/Control Assembly

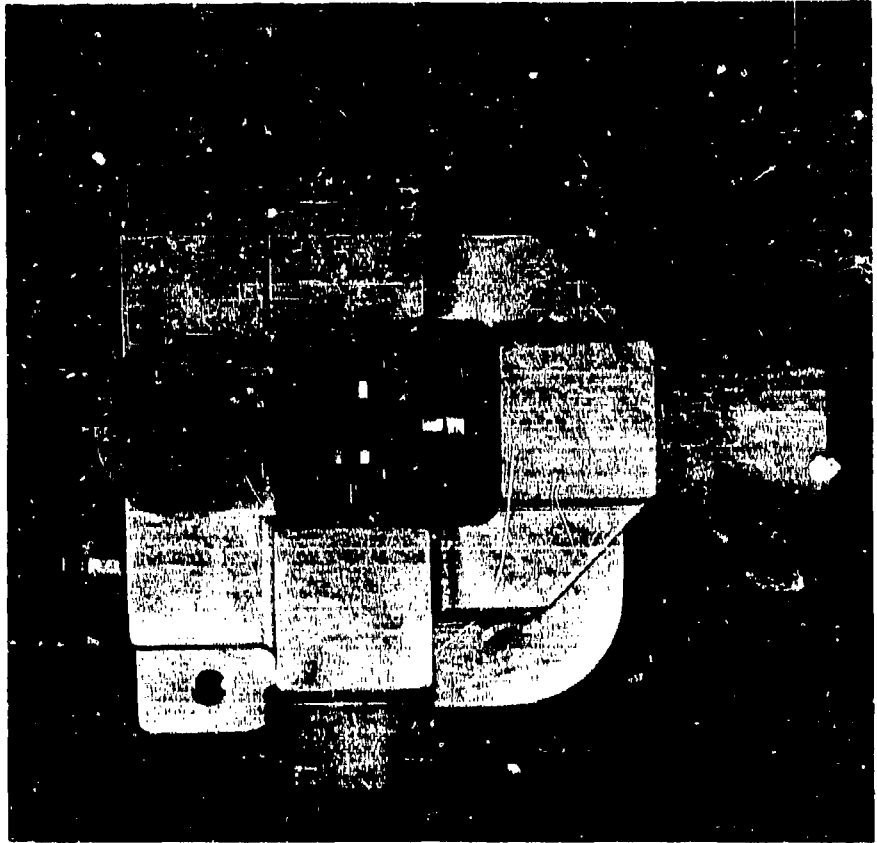


Figure 38. End View of Thrust/Control Assembly



Figure 37. Tube Bundle Assembly with Low Pressure Tubes Separated



Figure 38. Complete Tube Bundle Assembly

During this construction, a sample tube assembly was built duplicating the manifolding in the back and front. This unit was then subjected to hydrostatic testing.

A. CORROSION AND RUST INHIBITING

Before any hydrostatic testing could be accomplished, a decision had to be made relative to the most practical and least expensive corrosion inhibiting procedure. Internal nickel plating was considered but two drawbacks were noted: (1) this would be a very expensive operation with no assurance that under repeated cyclic pressurization the cracks in the nickel plating surface would not develop, thereby defeating the purpose of the inhibiting procedure; and (2) it was pointed out by personnel in the Stress Department that any rupturing of the nickel plated surface would most likely occur at the most critical point at the front where the plugs were welded into the end of the tube.

It was thus decided to use a very light rust inhibiting oil and thoroughly oil the inside of the tubes under operating pressures. Since only dry nitrogen gas would be used, it was felt that no explosion hazard would exist unless extreme temperatures were reached during pressurization.

The sample tube was next hydrostatically tested in the laboratory; the first test was the proof pressure test. The purpose of this test was to determine the volumetric set. The sample tube bundle was tested according to LTR 61-R-27 and was pressurized in increments of 250 psig and ultimately to 3150 psig proof pressure. 1500 psig was used as a base for set readings. 3150 psig was held on tube bundle for five minutes. No leakage or drop in pressure was observed. The volumetric set was 0.04 percent. The sample tubes were then hydrostatically cyclic tested 20,000+ times where the minimum pressure was 180 psig and the maximum was 2180 psig. At the higher pressures, a dwell time of approximately 3 seconds was used. The total cycle occurring approximately every 7 seconds.

Following this test, the sample tube assembly was subjected to higher hydrostatic pressures and finally burst at 9500 psig. No leaks were observed until burst. The burst occurred in a straight portion at the forward end of the tube and was in the form of a longitudinal fracture. Figure 39 shows the tube section used in this test.

After these tests, the high pressure and low pressure tubes of the Zero-G Belt were subjected to the following tests. The high pressure tube bundle was pressurized to proof pressure equivalent to 3150 psig using 1500 psig as a base pressure. There was a 0.04 percent set observed. The tube bundle was cycled ten times from 250 to 2500 psig. No leaks were observed in the tube lines and/or sealings. Aluminum low pressure tubes were proof tested to 500 psig. As in the other tubes, no leaks were observed. Before complete assembly, other units in the system were likewise separately and suitably tested to assure a maximum safety factor. These items were the pressure regulator, filter, manual shutoff control, and controller assembly.



Figure 39. Test Tubes Showing High Pressure Rupture

B. ASSEMBLY

The inside of the tube bundles were lined with three layers of fiberglass bonded to the tubes themselves. The fiberglass layer served two purposes: (1) attachment of bodice filler material; and (2) provided an additional safety feature for the operator. During the operation of lining the tube bundles with fiberglass, suitable attachment points were provided for the shoulder and leg straps. Also, an attaching bracket was installed that provided mounting for the controller assemblies.

The next operation was that of completing the installation of the plumbing, regulator, shutoff valve, filter, low pressure burst disk, thrust nullifier assembly, and the controller valves. Figures 40 and 41 show the completed assembly.

It is to be noted at this point that owing to the R&D nature of this device, as previously pointed out, some trouble was experienced in sticking and dragging during operation of the controller valves. It was discovered that any distortion created within the controller assembly as a result of mounting to the tube bundle assembly amplified and aggravated the sticking conditions within the controller. This sensitivity on the part of the controller necessitated a design change to a different type of mounting of the controller to the tube bundle assembly. This change was incorporated in the form of a flanged heavy mounting plate attached to the tube bundle assembly and provided rigid mounting for the controller. Upon completion of final assembly, the Zero-G Belt was pressurized to 2150 pounds, using dry N_2 gas. After two or three operational cycles including minor adjustments, cleanup, etc., the belt was ready for operational testing.



Figure 40. Front View of the Zero-G Belt

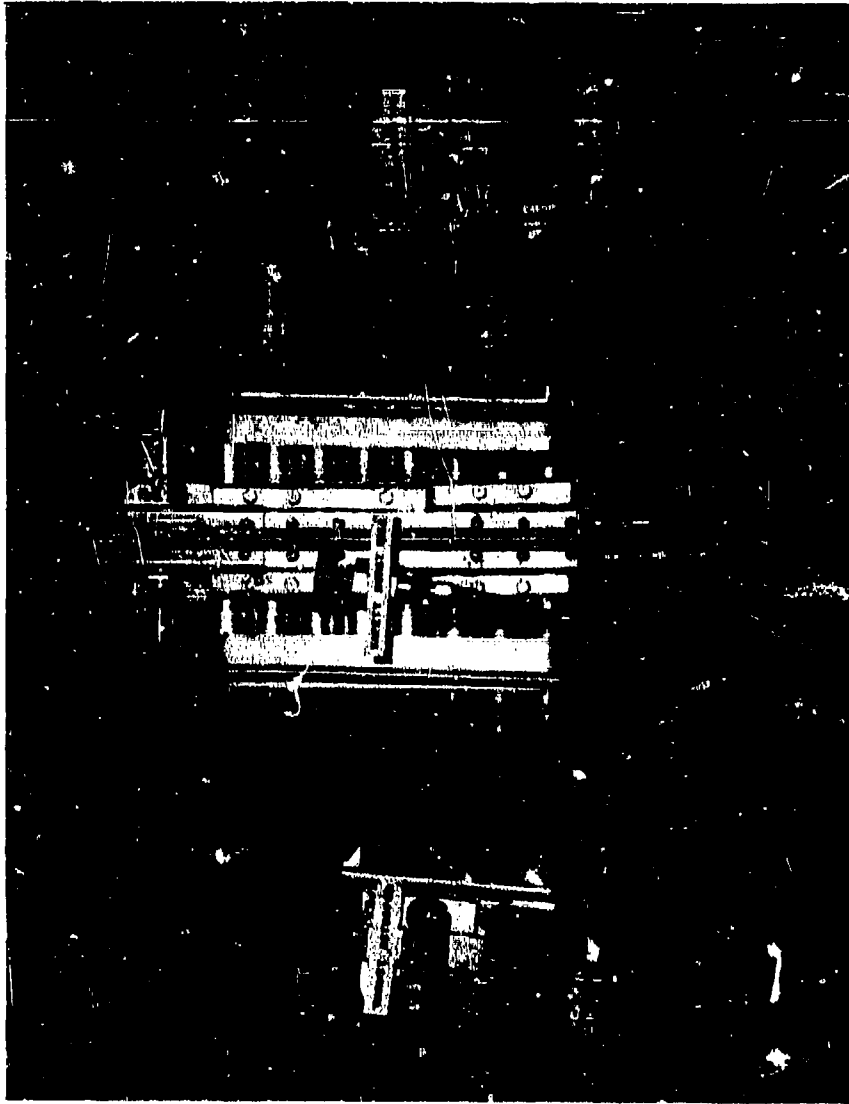


Figure 41. Rear View of the Zero-G Belt

SECTION VI. ZERO-G BELT TEST AND EVALUATION

A. AIR BEARING PLATFORM TESTS

Functional testing of the completed unit was initiated in March 1961, using Bell's air bearing platform. The first "flights" on the air bearing platform were used to assess the effectiveness of the propulsion and control system as well as to provide training for personnel scheduled to use the belt in the C-131 flight testing program. Due to a scheduling problem affecting the availability of test time in the C-131, tests on the platform to accurately measure the thrust output of the paired units were deferred until after the initial flight tests in the C-131. However, all of the platform testing is described in this section.

The Bell air bearing platform facility consisted of a smooth level surface of 1-1/2 inch masonite that measured 12 x 24 feet. Factory air was supplied by an overhead air supply brought down to a chamber on a plywood platform where it was equally distributed to three levitation pads. The overhead arrangement of the air pipes and connections resembled a pantograph type of design that made it possible for the plywood disk to move to any point on the floor without binding, friction, or encumbrance. Total friction involved in moving the platform was measured to be less than 1/2 ounce. The platform was free to rotate in either direction, translate fore and aft, left and right, or rotate and translate simultaneously. By use of this basic facility and placing the belt and operator in either a vertical or horizontal position, performance under any three of the six degrees of freedom could be assessed. Figure 42 shows the spaciousness of the facility and Figure 43 shows the facility being used for operator training.

The design goal of the Zero-G Belt Program was to fabricate a unit capable of producing a total thrust of more than 20 pounds in any direction using a chamber pressure of 185 psig in a vacuum environment. Two size nozzles were utilized; the smaller of the two was to produce 5 pounds of thrust and the larger 10 pounds. By pairing two ten pound thrusters, each located at the same point with respect to the man's cg, but on opposite sides, translational and rotational thrusts of twenty pounds were anticipated. The smaller units were also paired, but two were located on each side of the belt. These units were used for providing vertical translation, rotation or roll about the operators longitudinal axis and rotation or pitch about the horizontal axis. Figure 39 shows the location of these units. By separating these units, hand room on the controller was made possible and ten pounds of pitch force on each side could be generated. Although it was recognized that the lever arm produced by this design was greater for rotation about the vertical axis (yaw) and the longitudinal axis (roll) than for rotation about the horizontal axis (pitch), it was assumed that the operator could compensate for the differences in rotation rate by differential thrust duration.

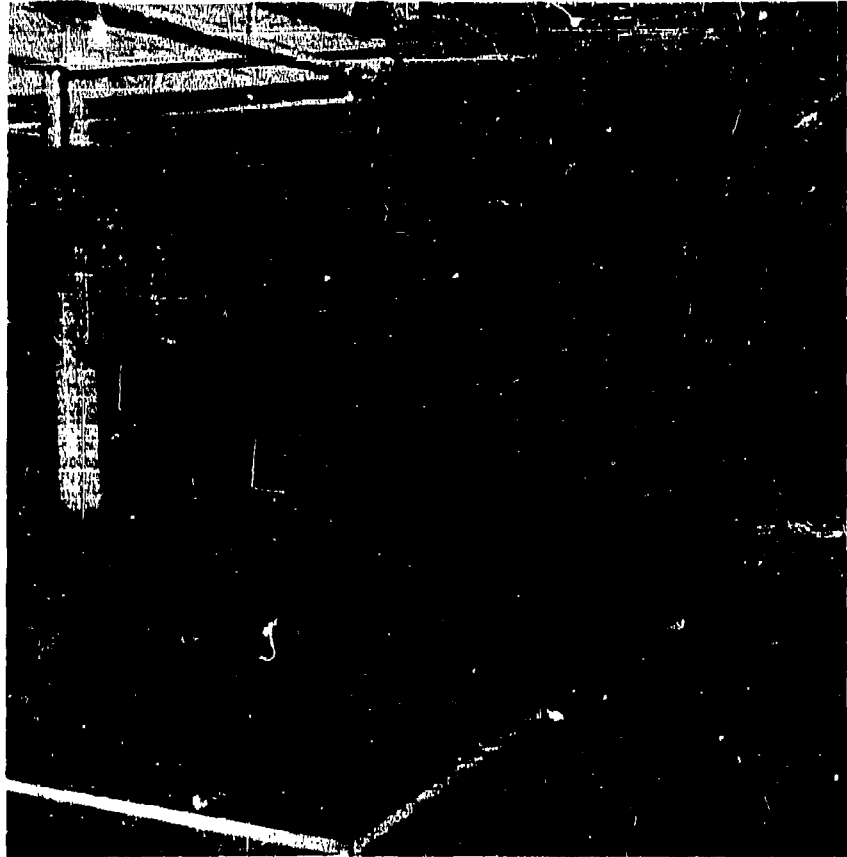


Figure 42. The Bel' Air Bearing Platform

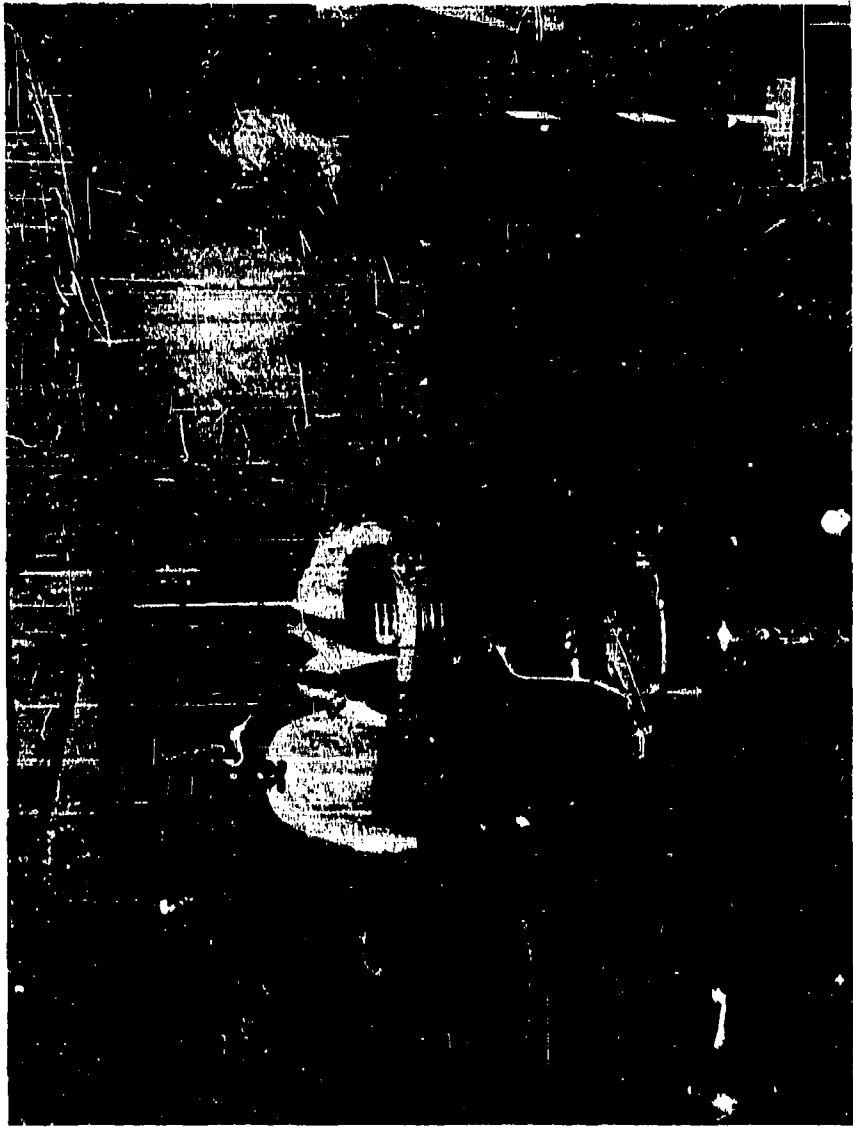


Figure 43. Zero-G Belt Training On The Air Bearing Platform

Shortly after the second series of flight tests in the C-131 aircraft, it was decided that more accurate measurements of yielded thrust should be taken. Up to this point, and with the exception of the original thrust tests, thrust measures were taken on the air bearing floor using a "fish scale." For this series of measures a more accurate technique was identified but which also used the air bearing floor as a floating fixture. A calibrated load cell was mounted securely to one of the building columns at a distance above the floor to coincide with the axis of thrust of the belt nozzles. Two tie points on opposite sides of single or paired nozzles were tethered to a whiffle tree on the load cell using light cord. A third line along the axis of the load cell was run from the far side of the belt to a bulkhead mounted pulley so that a steadying preload could be applied. This is depicted in Figure 44. The setup used for other thrust conditions is shown in Figure 45. A variable range potentiometer recorder with a chart speed of 1 inch per second was used for all measurements.

Initial tests were made with a man riding the platform to actuate the belt controls. This method proved to be unsatisfactory because it introduced perturbations in output with peak amplitudes in the order of 2 pounds. Ingenuity on the part of the technicians provided a simple but effective "rubber band" actuator with a sensitive trip lever to replace the man. This technique was used in obtaining the tabulated result presented in Table III.

Inspection of the results indicates that the actual operating thrust generated by the system varied from one set of nozzles to another and in several instances was well below the design thrust. For example, a total thrust of 11.18 pounds were generated for forward translation and 10.45 pounds for rearward translation. For yaw left, 10.57 pounds were generated. For a left roll, 11.82 pounds of thrust were generated. For vertical translation, 8.25 pounds up and 9.21 pounds downward were generated.

The low yield of thrust of the fully functioning system as compared to the initial testing of the nozzles was attributed to starvation of the thrust chambers due to limitation of the regulator, in keeping the low pressure tubes fully pressurized. In order to further increase the yield thrust, an additional regulator was placed on the opposite side of the belt, larger connecting hoses and tubes were used, and the pressure in both the high and low pressure tubes was increased. Whereas the original pressures were 2150 and 320 psig, they were raised to 3000 and 350 psig, respectively. After those modifications were made, thrust measures for just the translational forces were made. The net increase was about 4 pounds giving a yield thrust of approximately 15 pounds.

B. FLIGHT TESTS

Three series of flight tests were performed in the aircraft during the months of April, August, and November of 1961. During these tests, the belt was flown a total of 106 zero-g parabolas; 40 in the first series, 41 in the second, and 25 in the third. Subject operators included both Bell and Air Force personnel. The flights flown in



Figure 44. Thrust Testing of the Air Bearing Platform.

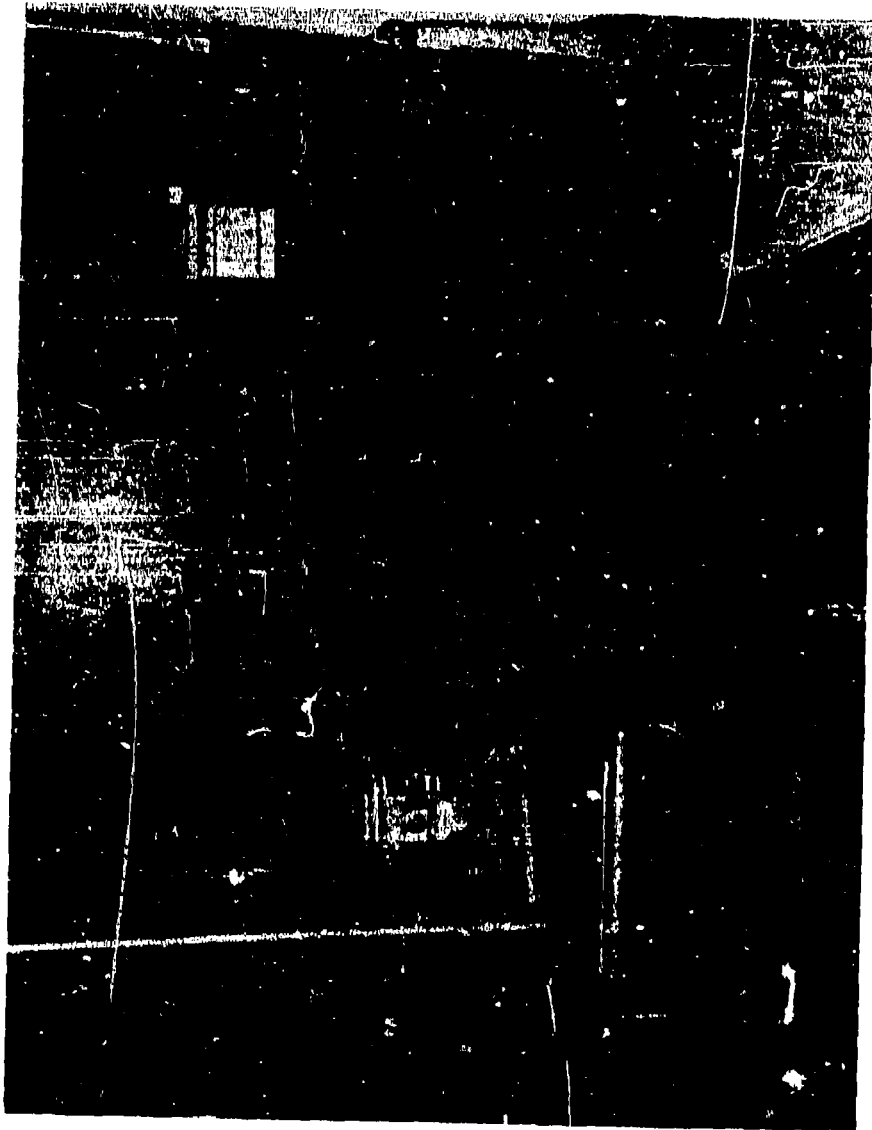


Figure 45. Close-up of Thrust Testing Rig

TABLE III
THRUST LEVELS MEASURED ON THE ZERO-G BELT

<u>Thrust Direction</u>	<u>Nozzles</u>	<u>Thrust</u>
1. Astern	RH	5.05
2. Astern	LH	5.4
3. Forward	RH	5.61
4. Forward	LH	5.52
5. Right	LH	7.56
6. Left	RH	7.59
7. Downward	A11	9.21
8. Downward	LH	5.73
9. Downward	RH	3.57
10. Upward	RH	6.09
11. Upward	LH	5.4
12. Upward	A11	8.25
13. Astern	A11	-
14. Forward	A11	-

the first series were exploratory in nature and used total thrusts in each axis of approximately five pounds. During these flights, photographic records provided the only data taken other than subjective comments of the flight crew. Control was demonstrated in all axes of rotation and directions of translation, but the thrust levels were considered to be too low to satisfactorily control the desired maneuvers in the 15 to 20 second period of weightlessness or to compensate for the aircraft movement toward the test subject when it is flying less than a perfect parabola. As a result of the experience gained during this first series of flights, it was decided to reset the regulators and increase the total thrust of the paired units and to conduct further tests.

During the second series of test flights, a total thrust of approximately nine pounds in each axis was used. Two Air Force subjects participated in these flights, and each of the subjects was given detailed instructions prior to attempting to fly a given maneuver. The tests conducted during this series of flights were rigidly structured and specific translation and rotation maneuvers were attempted. Table IV presents a listing of the maneuvers which were attempted. Due to the limited availability of the test aircraft, each subject was given only one trial on each maneuver except where inadvertent accelerations as a result of turbulence or an imperfect parabola were of a magnitude that made it impossible to attempt the maneuver. In these cases (5 parabolas of the 41 flown) the subjects were given a second chance at the maneuver. It is recognized that one trial opportunity to learn to control a new system through a defined maneuver in an unusual environment does not permit much learning. However, the decision was made to fly as many different maneuvers as possible during this series of tests and to attempt to optimize the difficult maneuvers during subsequent flight test programs.

Each maneuver was broken down into significant parts and scored for success of completion. The total maneuver performance was also rated. Complete motion picture coverage of each maneuver was provided. Figure 48 shows one subject attempting a translation during the weightless period. At the conclusion of each parabola, the ratings were made jointly by the operator and a trained observer on each part of the maneuver. Tables V and VI present the test record sheets for a typical maneuver.

TABLE IV
MANEUVER SCHEDULE FOR ZERO-G BELT FLIGHT TEST

1. Forward translation from a vertical position
2. Reverse translation from a vertical position.
3. Lateral translation from a vertical position.
4. Forward translation from a prone position.
5. Reverse translation from a prone position.
6. Vertical translation up and down from sitting position.
7. Rotation, 360° left and 360° right around vertical axis.
8. Rotation, 360° forward and 360° backward around horizontal axis.
9. Rotation, 360° left and 360° right around longitudinal axis.
10. Zero-g walk on floor.
11. Zero-g walk on wall.
12. Zero-g walk on ceiling.
13. Zero-g walk around cabin.
14. 90° Change in pitch during forward translation.
15. 90° Change in roll during forward translation.
16. 90° Change in yaw during forward translation.
17. Straight translation from vertical position, stop, 180° yaw turn, return to starting point.
18. Straight translation from prone position, stop, 180° pitch rotation and 180° roll and return to starting point.

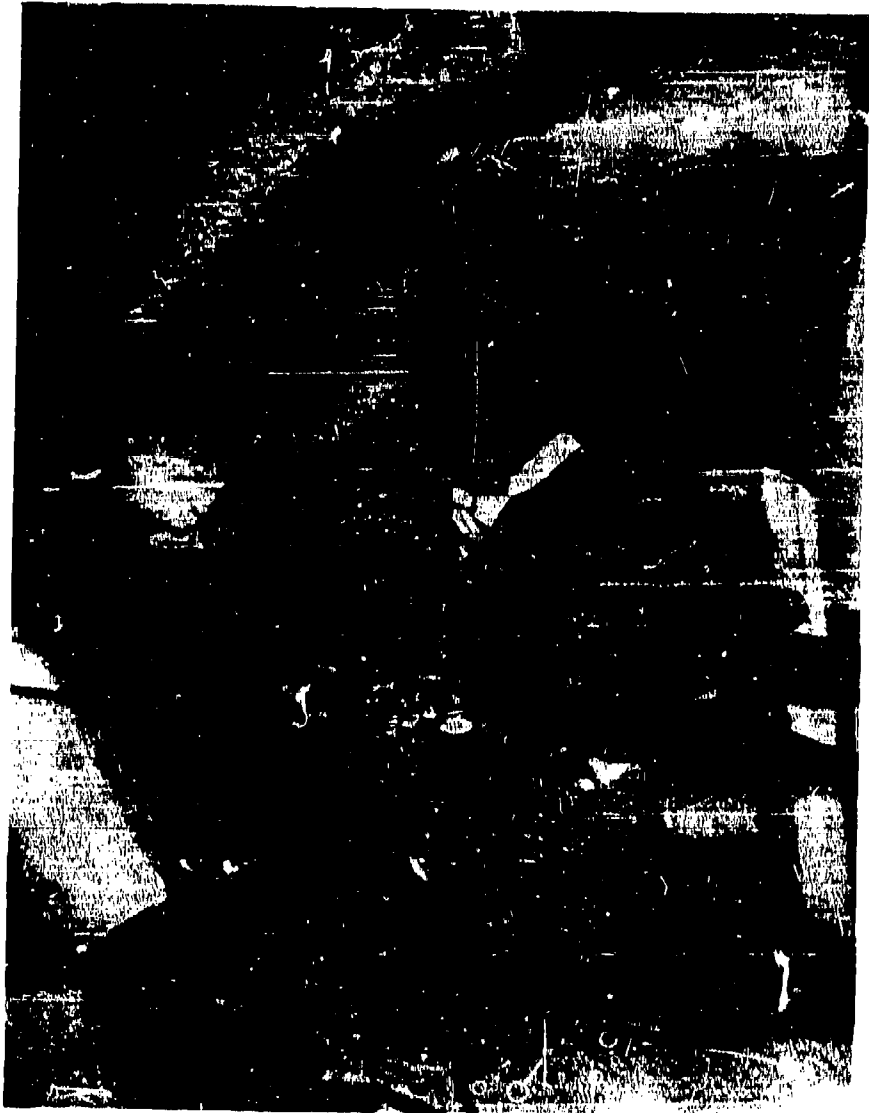


Figure 46. Zero-G Belt in Flight

TABLE V

ZERO-G BELT FLIGHT TEST RECORD

MANEUVER NO. 1 "Forward Translation from Vertical Position"

A B C D E F G H

ITEM:	Poor	Fair	Good	Ex.
a. START	<input type="checkbox"/>	<input type="checkbox"/>	<input type="checkbox"/>	<input type="checkbox"/>
b. RATE	<input type="checkbox"/>	<input type="checkbox"/>	<input type="checkbox"/>	<input type="checkbox"/>
c. STABILITY	<input type="checkbox"/>	<input type="checkbox"/>	<input type="checkbox"/>	<input type="checkbox"/>
d. ATTITUDE CONTROL	<input type="checkbox"/>	<input type="checkbox"/>	<input type="checkbox"/>	<input type="checkbox"/>
e. DIRECTION CONTROL	<input type="checkbox"/>	<input type="checkbox"/>	<input type="checkbox"/>	<input type="checkbox"/>
f. RANGE CONTROL	<input type="checkbox"/>	<input type="checkbox"/>	<input type="checkbox"/>	<input type="checkbox"/>
g. OVERALL RATING	<input type="checkbox"/>	<input type="checkbox"/>	<input type="checkbox"/>	<input type="checkbox"/>

(Value)

1 2 3 4 5 6 7

COMMENTS

Item:

- a. _____
- b. _____
- c. _____
- d. _____
- e. _____
- f. _____
- g. _____

Other _____

QUALITY OF PARABOLA _____

OBSERVER

OPERATOR

NAME _____

DATE _____

TABLE VI
MANEUVER AND SCORING INSTRUCTIONS
(Maneuver No. 1)

Start from kneeling position. At zero g, use sufficient down thrust to lift off floor. Apply forward thrust accelerating to desired speed. Coast using corrective thrust for position control. Apply reverse thrust early enough to stop at end of cabin.

A. SCORING

Item:

- a. Excellent performance is positive liftoff to approximately 2-foot clearance of knees to floor.
- b. Excellent performance is rapid (2-second) acceleration to acceleration to desired translational speed.
- c. Excellent performance if operator maintains forward orientation and vertical body position.
- d. Excellent performance if operator can make adequate corrections in flight to maintain body orientation in pitch, yaw, and roll.
- e. Excellent performance if operator is able to apply reverse thrust to stop at desired point.
- f. Excellent performance if accurate control of flight path is accomplished.
- g. Overall maneuver performance.

B. OTHER

Please comment on all characteristics of belt related to performance, i.e., thrust level, control sensitivity, and location - suggestions for improvement.

Table VII presents the estimated percent of successful completion for each maneuver on the second test series. While it is not possible to attach any statistical significance to the data found in Table VII, some trends can be noted and used as hypotheses for further study or comparisons.

TABLE VII
ESTIMATED PERCENT SUCCESS OF EACH MANEUVER

<u>Maneuver Number</u>	<u>Operator No. 1</u>	<u>Operator No. 2</u>
1	90	75
2	50	75
3	75	75
4	90	100
5	10	25
6	90	100
7	100	80
8	25	50
9	100	100
10	25	100
11	10	25
12	10	10
13	5	90
14	75	75
15	10	50
16	25	60
17	0	100
18	80	-

The first six maneuvers were straight translations. Of these six translations, only maneuver number 5, reverse translation from a prone position, offered serious difficulty. This difficulty should not be surprising, however, when the nature of the maneuver is considered. In the rotational maneuvers (7, 8, 9,) only maneuver 8, rotation in the pitch axis, demonstrated poor completion success. The zero-g walks, maneuvers 10 to 13, also indicated fairly poor success. It is likely that forces produced by the flexion of the ankle during the walking was greater than the approximately nine pounds of thrust provided by the propulsion system and therefore the operators were actually forcing themselves away from the surface on which they were trying to walk. The results of maneuvers 14 to 18 indicate that the attempt to engage in simultaneous control of both translation and rotation yields relatively low percentage of success. Table VIII presents the mean operator ratings for each maneuver component, averaged across the 18 different maneuvers.

TABLE VIII
MEAN OPERATOR RATINGS OF EACH MANEUVER COMPONENT

<u>Component</u>	<u>X Operator No. 1</u>	<u>X Operator No. 2</u>
Start	4.87	4.72
Rate	4.44	3.78
Stability	3.58	3.50
Attitude Cont.	3.72	4.12
Directional Cont.	4.23	4.31
Range Cont.	4.10	4.00
Overall Rating	4.22	3.88

* A value of "7" is maximum and "0" minimum, "3.5" is between "good" and "fair."

These ratings indicate that the test operators rated each of the maneuver components at a level which indicates fair to good control. It is important to note that these ratings, when compared to other zero-g propulsion systems tested in the Aerospace Medical Laboratory aircraft, indicate that the system offers considerable performance improvement over the other systems.

The third and final flight test series used a configuration of the zero-g belt that yielded total thrusts of slightly over 15 pounds. Since it was known that the number of parabolas to be flown would be limited, it was decided to repeat all maneuvers on which the belt was rated either low or unsatisfactory on the previous test series. These, including their new rating, are given in Table IX.

TABLE IX
PERFORMANCE RATINGS ON THE ZERO-G BELT

<u>Maneuver Number</u>	<u>Description</u>	<u>Rating</u>
5	Reverse translation from a prone position	75
8	Rotation, 360° forward and 260° backward around horizontal axis	75
9	Lateral Rotation	75
11	Zero-g walk on wall	25
12	Zero-g walk on ceiling	75
15	90° change in roll during forward translation	50
16	90° change in yaw during forward translation	75
18	Straight translation from prone position, stop, 180° pitch rotation, 180° roll and return to starting point.	75

The results of this test series were most encouraging and gave evidence that with practice, and when a good parabola was flown, any of the 18 maneuvers could be performed satisfactorily with the belt at the new thrust levels.

SECTION VII. CONCLUSIONS

In spite of the lack of precise performance data we are of the opinion that the following conclusions obtained from the development and test of the Bell Zero-B Belt are warranted:

- (1) The belt, in its current configuration, has demonstrated an encouraging capability to translate and rotate a man in a weightless environment.
- (2) A two-hand controller is not desirable. It has been determined that a single-hand controller is necessary so that the second hand is free for other functions, and to assure an equal thrust application on both sides to prevent unintentional rotation.
- (3) Throttleable thrust is required. The operator should be able to vary the thrust output over the entire range of thrusts possible. It is important that the thrusts utilized for rotational control be optimum for each axis because of the different moments of inertia present in each axis.
- (4) Because of the short exposure to zero g during any one parabola, and because of the disturbances induced by turbulence and imperfect trajectories, it was not possible to assess man's capability to stabilize himself without some augmentation. Although later experience with the Mercury capsule indicates automatic stabilization wastes fuel, the case for, against, or a compromise position cannot be made on the basis of these test results.
- (5) It is recommended that future testing of a manned propulsion system for a space worker be conducted in a six-degree-of-freedom simulator where greater freedom and duration of performance can be obtained. In the event that more suitable aircraft and autopilot programmers are developed to generate more zero-g time, maneuvering space, and quality of parabolas, further aircraft testing may prove valuable.
- (6) Various techniques have been devised and tried for assessing an operator's performance when attempting to do specific maneuvers in the C-131 under conditions of weightlessness. These have included introspection, written or verbal recordings by an observer, and motion pictures. Objective and subjective assessment has proven very difficult thus far due to the extraneous and unrecorded accelerations imparted to the air mass in the cabin that overwhelm the performance of a propulsion unit. The effect of these extraneous accelerations made analysis of the motion picture impossible.

Their effects on the observer recordings and the introspective reports are not known. Until such time as perfect parabolas can be flown consistently, it is doubtful that even an automatic recording system would be useful. Until this time, it is suggested that the use of performance record sheets, filled in by trained observers who can allow for the extraneous disturbances, be utilized.

SECTION VIII. RECOMMENDATIONS

The introductory section of this report presented the context within which the development and test of the Bell Zero-G Belt took place. It was pointed out that the orderly development of an operational system for augmenting a space worker's capability would require research and study on all related problem areas. Although this report is primarily concerned with the development and test of the belt, we have included specific recommendations for additional work in all associated fields of interest.

As indicated, the development of an optimum self-maneuvering unit for the orbital worker should be directed toward the integration of the required life support systems, propulsion system, stability and control system, and support systems necessary for the required orbital activities. The successful and timely development of the orbital worker system will require expanded research plus development studies in a number of areas. Figure 47 presents, in summary form, a recommended study plan. The technical study effort has been divided into four major study areas; maintenance task parameters, orbital worker control capabilities, orbital worker environmental parameters, and stability control and propulsion concepts. The discussion that follows presents some of the more important research questions that must be thoroughly studied to accomplish the optimum development of the orbital worker system in each of the major study areas.

A. MAINTENANCE TASK PARAMETERS

All inspection, repair, replacement, servicing and assembly activities which may take place in the orbital environment have been grouped in the maintenance study area. The following areas represent some of the major problems yet to be solved:

- (1) Classes of maintenance activities required.
- (2) Level of maintenance which will be attempted.
- (3) Design for maintainability in space for orbital systems.
- (4) Tool requirements for the predicted maintenance tasks.
- (5) Torques and linear forces which must be applied to complete the predicted activities.
- (6) Specification of fastening techniques which will be employed.
- (7) The levels of remoteness which will be required for maintenance.

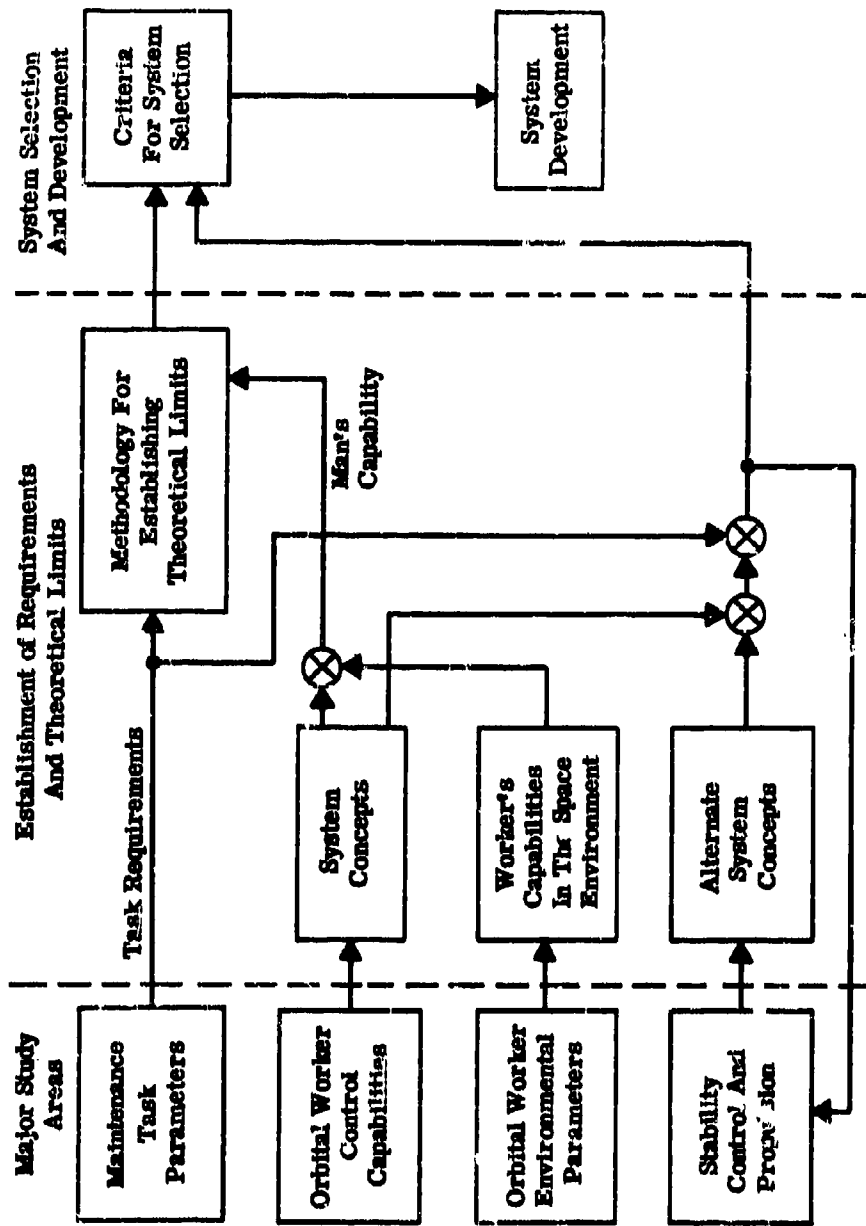


Figure 47. Orbital Worker Systems Study Plan

To achieve answers to these questions, predictive and detailed task analysis studies and task classification schemes must be developed. These should entail thorough engineering analyses of the predicted systems, subsystems, and components for each of the orbital systems and require the positioning of the best approaches to accomplishing the required maintenance. While a number of studies have been conducted in this general area, they have been concerned, for the most part, with theoretical analyses of the role of the man in orbital maintenance (4, 6, 10, 11). They have not emphasized the more mundane, but more critical, problems of what maintenance must be accomplished and what equipments are required to accomplish it.

B. ORBITAL WORKER CONTROL CAPABILITIES

In this area, the concern is with the problems related to the capability of the orbital worker to translate, with control, in the orbital environment. The criteria which must be employed to evaluate the translational performance are those concerned with the degree of control, the rate of expenditure of propellants, and life support system constituents. Large study efforts in each of the following problem areas must be undertaken:

- (1) The accuracy with which the orbital worker can orient his reaction control nozzles and control his thrust so that an optimum translation trajectory is achieved.
- (2) The accuracy with which the orbital worker can activate the control system so that rendezvous is accomplished with a minimum ΔV and a minimum rotation rate.
- (3) The resultant rotations in each of the three axes when thrusts are applied other than through the center of mass of the orbital worker system. Can the man adequately control these rotations or will his manual control attempts drive the system into severe oscillation?
- (4) Determination of the best techniques to employ when using manual control; one axis at a time or multiaxis controls.
- (5) The accuracy with which the orbital worker can judge closing rates and durations in the orbital environment. Are auxiliary systems required to present distance and relative velocity or can the orbital worker judge, with the required accuracy, these aspects of the visual environment?
- (6) The training which is required to yield satisfactory control of the orbital worker system.

C. ENVIRONMENTAL PARAMETERS

The study here should be directed toward two effects of the orbital environment on the design of the orbital worker system: the probability, nature, and results of equipment malfunction as a consequence of the environment and the requirements imposed by the environment on the design of the orbital worker system. The major problem areas are:

- (1) High vacuum effects on the external structure of the orbital worker system.
- (2) Maintenance of an appropriate thermal radiation balance within the orbital worker system.
- (3) Protective requirements for shielding the worker from galactic, solar cosmic, albedo cosmic, and particle radiation.
- (4) Protection against penetration or erosion resulting from micrometeorite bombardment.
- (5) Analysis of the visual environment as it poses requirements for protecting the worker, augmenting his visual skills and spatial orientation.

D. STABILITY, CONTROL, AND PROPULSION CONCEPTS

The only propulsion system designed for translation of the orbital worker on which data was available for consideration in this report was the Bell Zero-G Belt described in the previous sections of this paper. It is important to note, however, that this system, being a feasibility model, has only been capable of studying a very few of the many problems involved in the translation, with control, of an orbital worker. The source of thrust, compressed nitrogen gas, is certainly not the propellant which will be utilized in the orbital environment. Its thrust duration of approximately 11 seconds is certainly not sufficient to translate the worker with adequate fuel reserve over any realistic operational distances. However, in spite of these limitations, we now feel that we can speak positively from our experience with this system, and specify the additional studies which are required to develop an optimum propulsion system. The following study areas reflect our thinking to date in regard to this problem:

- (1) Thrust requirements and the control which the orbital worker should have over the amount and rate of thrust generated.
- (2) Optimal placement of thrust units, the disparities which can be tolerated, and the advantages of a few gimballed units over a larger number of fixed units.
- (3) Man/control system links which can be used; e.g., complete kinesthetic control, use of the lower limbs or other body segments, electronic controls using muscle potentials for signal inputs, etc.

- (4) Flexibilities which can be built into the propulsion system that will make it possible to use the same basic system in different gravitational fields; i.e., orbital and lunar.
- (5) Optimum propellant to use in a system with respect to storability, specific impulse, density, vapor pressure, toxicity, leakage tendency, erosiveness, availability, controllability, ease of handling, and maintenance requirements.

E. APPROACHES TO STUDY

Investigation of the performance characteristics of any orbital work system concept requires the simulation with a high degree of realism of the unique effects of the zero-g environment. Three different approaches to this simulation problem have been extensively studied during the recent years: (1) water immersion; (2) three-degree-of-freedom air bearing (frictionless) devices; and (3) Keplerian trajectories.

1. Water Immersion

Water immersion techniques have been used primarily in an attempt to provide an environment which compensates for the earth's gravity by suspending a subject in water which has approximately the same specific gravity as the human body. Any study of the response capability of the subject to perform in this environment for the evaluation of any proposed propulsion or stability, and control systems will be severely restricted by the damping effects of the water. Therefore, this approach does not offer the capability of studying the dynamic performance of any orbital worker system or determining the capability of the operator to control the system in the orbital environment. For limited studies of task accomplishment at a work site, however, this technique appears to be useful.

2. Three-Degree-of-Freedom Air Bearing Devices

There are a number of devices in existence in this country capable of simulating the dynamics of weightlessness in two dimensions. Such air bearing platforms simulate two translational degrees of freedom (lateral and fore/aft), and one rotational degree of freedom. These devices, while valuable in studying limited performance of propulsion, stability, and control systems, do not enable the valid study of the capability of the human to function in the weightless state simultaneously in all six degrees of freedom. The validity of extrapolation of data collected on such devices to six-degree-of-freedom problems must be questioned for a basic reason. All of the dynamic effects of a force exerted in a given axis are translated into the planes of frictionless motion and do not validly represent the responses that would occur if all translational and rotational axes were frictionless. Thus, the interpretation of the resultant responses of a body located on a two-dimensional air bearing platform must be regarded as suspect.

Another class of three-degree-of-freedom devices which is capable of simulating the inertial effects of weightlessness is represented by the MASTIFF, located at NASA, Lewis Research Center. This facility while valid for studying the capability of the astronaut in damping spins in up to three rotational axes, offers no capability for studying the ability of the astronaut to simultaneously control both the translational and rotational degrees of freedom.

In summary, the three-degree-of-freedom air bearing devices offer the capability of collecting preliminary information to questions centered around the capability of the human to translate and control movements in the weightless environment. They do not offer the capability of answering the critical problems which are present in the true six-degree-of-freedom case.

3. Keplerian Trajectories

Such trajectories performed in an aircraft of a size sufficient to permit a man to maneuver in an unrestricted manner, offer 10- to 20-second periods of zero gravity in six degrees of freedom. Rotation in all three axes is possible but translation distances are restricted by the physical dimensions of the aircraft interior which must remain small. Also, extraneous accelerations of the air mass within the cabin of the aircraft are induced when turbulence is present in the atmosphere during the parabola or when pilot technique is less than perfect. These induced accelerations greatly effect the ability of the man to perform translational or rotational maneuvers and thereby project unknowns into the research data. In addition, the effects of the relatively high gravity fields, both prior to and immediately following the zero gravity period, may significantly affect the capability of the subject to perform during the zero gravity period.

In spite of these shortcomings, the simulation of zero gravity during aircraft trajectories must be considered the best medium currently available for simulation of the frictionless effects of weightlessness on bodies. Furthermore, the programmed use of the Lockheed C-130 by personnel of the Aerospace Medical Research Laboratory, will greatly increase the duration of the zero gravity trajectories and the translational distances capable of being simulated. However, the time restriction which is imposed by simulating zero gravity in this manner must be regarded as a severe limitation on the use of this technique for research purposes. In addition, the cost of operating the aircraft during the flights is high and recurring, which places a severe financial load on a research budget.

4. Improved Simulation Approaches

Improved techniques must be developed for simulation of the frictionless aspects of the orbital environment. One approach that appears to offer the necessary simulation fidelity is a six-degree-of-freedom simulator. This device will enable valid study of the capabilities of the human to control performance in all axes during translation. Such a facility would enable study of a majority of the research problems listed above and would enable the precise collection of performance data during the evaluation process.

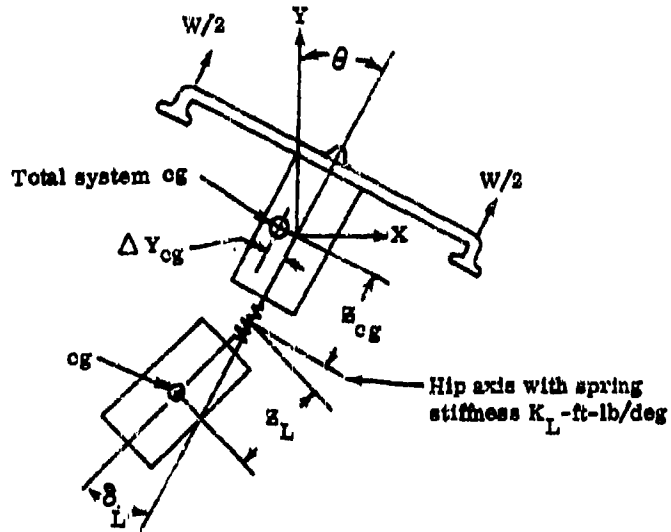
SECTION IX. REFERENCES

1. Bell Aerosystems Company Report No. 7052-953001, "Remora Manned Space Capsule Study," 1960.
2. Bell Aerosystems Company Report No. D7123-953001, "Self-Maneuvering Unit for Orbital Maintenance Workers," January 1961.
3. Bell Aerosystems Company Report No. D7142-953001, "Proposal for the Study of Space Maintenance Techniques," July 1961.
4. Bell Aerosystems Company Report No. D7181-953001, "Proposal for an Integrated Back-Pack Maneuvering Unit", August 1962.
5. Bond, N.A., "Maintaining Space Vehicles," ARS paper 1218-60, May 1960.
6. Dzendolet, E., and J.F. Rievley, "Man's Ability to Apply Certain Torques While Weightless", WADC TR 59-94, Wright Air Development Center, Wright-Patterson Air Force Base, Ohio, April 1959.
7. Griffin, J.B., "Feasibility of a Self-Maneuvering Unit for Orbital Maintenance Workers", ASD TDR 62-278, Aeronautical Systems Division, Wright-Patterson Air Force Base, Ohio, August 1962.
8. Grodsky, M.A., and R.D. Sorokin, "Man's Contribution to an Operational Space Station Concept", Proceedings of the Manned Space Stations Symposium, April 1960.
9. King, B.G., et al, "The Center of Mass of Man". TR NAVTRADEVCEEN 85, Naval Training Device Center, Port Washington, New York, November 1959.
10. Kornhauser, M., "Current Estimates of the Effects of Meteorites on the Skin of a Satellite Vehicle", Advanced Space Vehicle Engineering Memo 3, General Electric, MSVD.
11. Loftus, J.P., and L.R. Hammer, "Weightlessness and Performance, a Review of the Literature", ASD TR 61-166, Aeronautical Systems Division, Wright-Patterson Air Force Base, Ohio, June 1961.
12. McRuer, D.T., I.L. Ashkenas and E.S. Krengal, "A Positive Approach to Man's Role in Space", Aerospace Engineering, August 1959, 18, pp. 30-36.
13. Meister, D., and R.B. Wilson, "The Role of Man in the Maintenance of Earth Satellites", ARS paper 1214-60, May 1960.

14. Meyer, P., E.N. Parker, and J.A. Simpson "Solar Cosmic Rays of February 1956 and Their Propagation Through Interplanetary Space", *Physical Review*, Vol. 104, 1956.
15. Simons, J.C., and M.S. Gardner, "Self-Maneuvering for the Orbital Worker", WADD TR 60-748, Wright Air Development Center, Wright-Patterson Air Force Base, Ohio, December 1960.
16. Simons, J.C. and M.S. Gardner, "Personal Communication", August 1961.
17. Van Allen, J.A., "On the Radiation Hazards of Space Flight", Report No. SUI 59-7, State University of Iowa, May 1959.
18. Winkler, J.R., "Cosmic-Ray Increase at High Altitude on February 23, 1956," *Physical Review*, Vol. 104, 1956.

APPENDIX

SIMPLIFIED EQUATIONS OF MOTION
FOR SRLD - UNCONTROLLED



Moments @ total cg (Assuming No Motion Along Y)

$$\frac{I \ddot{\theta}}{57.3} = T \Delta Y_{cg}$$

$$\text{Since } W_{total} = T \text{ and } \Delta Y_{cg} = - \frac{W_L}{W_{total}} \cdot \frac{Z_L}{57.3} \cdot \delta_L$$

$$\text{Then } \frac{I \ddot{\theta}}{57.3} = - \frac{W_L Z_L}{57.3} \cdot \delta_L$$

Σ Forces along X

$$M_{total} \ddot{x} = \frac{W \theta}{57.3}$$

Σ Moments of Legs at Hip Axis

$$Z_L \left[M_L \ddot{X} - (Z_L + Z_{cg}) \frac{\ddot{\theta} M_L}{57.3} \right] = K_L \delta_L + \frac{W Z_L \delta_L}{57.3}$$

$$\text{or } M_L \ddot{X} - (Z_L + Z_{cg}) \frac{\ddot{\theta} M_L}{57.3} = \left[\frac{K_L}{Z_L} + \frac{W}{57.3} \right] \delta_L = \delta_L K'_L$$

These equations take the form

$$\ddot{\theta} + 0 \dot{X} + \left(\frac{W Z_L}{I} \right) \delta = 0$$

$$\ddot{\theta} + \left[\frac{-57.3}{(Z_L + Z_{cg})} \right] \dot{X} + \left[\frac{K'_L 57.3}{M_L (Z_L + Z_{cg})} \right] \delta = 0$$

$$\ddot{\theta} + \left(\frac{-57.3}{g} \right) \dot{X} + 0 \delta = 0$$

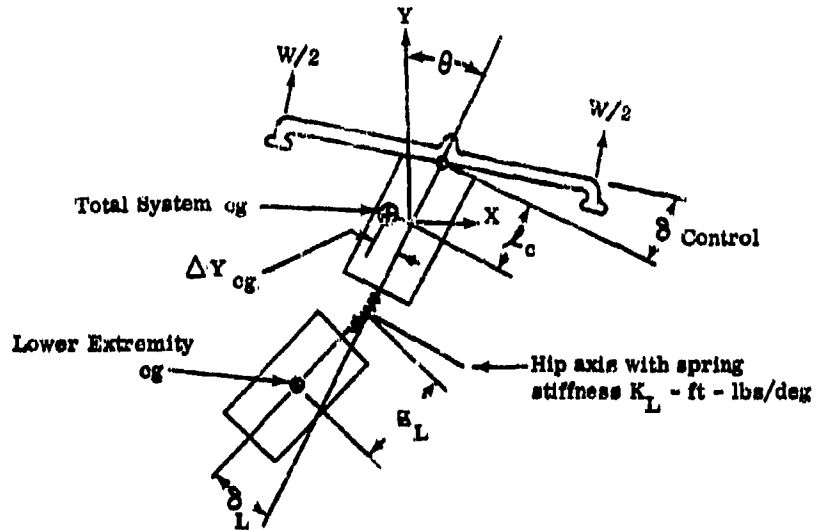
From solution of Laplace Transform

$$\frac{\theta}{\theta_0} = \cos \omega t$$

$$\text{Where } \omega^2 \approx \frac{W_L^2 Z_L}{57.3 K'_L I}, \quad \frac{X}{\theta} = A \sin \omega t$$

$$\text{Where } A \approx \frac{I K'_L g}{W_L^2 Z_L}$$

The simplified equations of motion with thrust vector control are as follows:



Moments at total og (assume no motion along Y)

$$\frac{1}{57.3} \ddot{\theta} = - \frac{W_L z_L}{57.3} \delta_L + \frac{W l_c}{57.3} \delta_c; \text{ where } \delta_c = -K \theta \text{ Pilot Control}$$

Σ Forces Along X

$$M_{\text{total}} \ddot{x} = \frac{W}{57.3} (\theta + \delta_c)$$

Σ Moments at Hip Axis (c° Legs)

$$z_L \left[M_L \ddot{x} - (z_L + z_{cg}) \frac{\ddot{\theta} M_L}{57.3} \right] = K_L \delta_L + \left(\frac{W_L z_L}{57.3} \right) \delta_L$$

or

$$M_L \ddot{x} - (z_L + z_{cg}) \frac{\ddot{\theta} M_L}{57.3} = \delta_L \left(\frac{K_L}{z_L} + \frac{W_L}{57.3} \right) = K'_L \delta_L$$

These equations take the form,

$$\ddot{\theta} + \left(\frac{W \ell_c K}{I}\right) \theta + 0 X + \left(\frac{W_L Z_L}{I}\right) \delta_L = 0$$

$$\ddot{\theta} + \left(\frac{-57.3}{Z_L + Z_{cg}}\right) \dot{X} + \left(\frac{K'_L 57.3}{M_L [Z_L + Z_{cg}]}\right) \delta_L = 0$$

$$\theta + \left(\frac{-57.3}{2(1-K)}\right) \dot{X} + 0 \delta_L = 0$$

Solution by Laplace transform yields

$$\frac{\theta}{\theta_0} = \cos \omega t$$

where

$$\omega^2 = \frac{W_L^2 Z_L (1-K)}{57.3 K'_L I} + \frac{K \ell_c W}{I}$$

$$\frac{X}{\theta} = A \sin \omega t$$

where

$$A = \frac{I K'_L g (1-K)}{W_L^2 Z_L (1-K) + W \ell_c K_L 57.3}$$

The torsio reference data for these equations is shown in Figure 48.

TORSO DATA (Reference WADC TR 55-159)

MEDIAN CLASS:

Total height = 69.5 inches

Distance from top of head to cg = 30 inches

Hip axis to bottom of feet = 35 inches

Hip axis to total cg = 4.5 inches

Hip axis to cg of lower extremities = 15 inches

Total weight = 164 pounds

Weight of lower extremities = 66.4 pounds

Moment of inertia (EET) = 20 slug ft² (This value has been corrected to 12.24 based on Ref. Aerojet Report.)

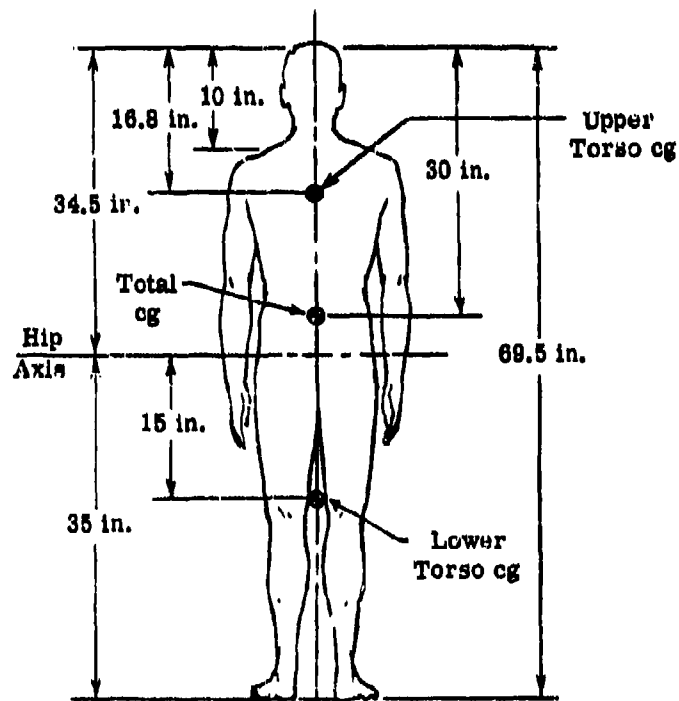


Figure 48. Torso Reference Data

<p>Aerospace Medical Division, 6570th Aerospace Medical Research Laboratories, Wright-Patterson AFB, Ohio Rpt. No. AMRL-TDR-63-23. DEVELOPMENT AND TEST OF THE BELL ZERO-G BELT. Final Rpt., Mar 63, vi + 103 pp incl. illus., tables, 18 refs.</p> <p>The assumption is made that a requirement exists for the development of a self-manuever- ing system for orbital workers. Such a sys- tem will consist of a life support subsystem, maintenance equipment (tools), and a propul- sion and control subsystem. This report dis- cusses the general problem areas and specifi- cally reports on the research, development, and testing of the Bell Zero-G Belt, a research propulsion and control system for maneuvering a man in a weightless environment.</p>	<p>UNCLASSIFIED</p> <ol style="list-style-type: none"> 1. Belts (zero-g) 2. Weightlessness 3. Orbital Worker 4. Rocket Propulsion 5. Control Systems 6. Space Vehicle <p>I. AFSC Project 7184, Task 71840E</p> <p>II. Behavioral Sciences Laboratory Contract AF33(657)- 9224</p> <p>IV. Bell Aerostystems Company, Buffalo, New York</p> <p>UNCLASSIFIED</p>	<p>Aerospace Medical Division, 6570th Aerospace Medical Research Laboratories, Wright-Patterson AFB, Ohio Rpt. No. AMRL-TDR-63-23. DEVELOPMENT AND TEST OF THE BELL ZERO-G BELT. Final Rpt., Mar 63, vi + 103 pp incl. illus., tables, 18 refs.</p> <p>The assumption is made that a requirement exists for the development of a self-manuever- ing system for orbital workers. Such a sys- tem will consist of a life support subsystem, maintenance equipment (tools), and a propul- sion and control subsystem. This report dis- cusses the general problem areas and specifi- cally reports on the research, development, and testing of the Bell Zero-G Belt, a research propulsion and control system for maneuvering a man in a weightless environment.</p>	<p>UNCLASSIFIED</p> <ol style="list-style-type: none"> 1. Belts (zero-g) 2. Weightlessness 3. Orbital Worker 4. Rocket Propulsion 5. Control Systems 6. Space Vehicle <p>I. AFSC Project 7184, Task 71840E</p> <p>II. Behavioral Sciences Laboratory Contract AF33(657)- 9224</p> <p>IV. Bell Aerostystems Company, Buffalo, New York</p> <p>UNCLASSIFIED</p>
<p>control system for maneuvering a man in a weightless environment. The flight tests of the belt took place on a large airbearing platform and in a C-131 cargo-type aircraft during zero-g trajectories. The equations of motion derived during the Bell Aerostystems Company sponsored development of the Small Rocket Lift Device (Rocket Belt) are also presented and discussed with respect to the Zero-G Belt. Specific conclusions are presented on the adequacy of the research model of a propulsion system and recommenda- tions are made for additional research and development</p>	<p>UNCLASSIFIED</p> <ol style="list-style-type: none"> V R. E. Fleeman, L. M. Seal C. Henderson VI. In ASTIA collection VII. Aval fr OTS: \$2.50 <p>UNCLASSIFIED</p>	<p>control system for maneuvering a man in a weightless environment. The flight tests of the belt took place on a large airbearing platform and in a C-131 cargo-type aircraft during zero-g trajectories. The equations of motion derived during the Bell Aerostystems Company sponsored development of the Small Rocket Lift Device (Rocket Belt) are also presented and discussed with respect to the Zero-G Belt. Specific conclusions are presented on the adequacy of the research model of a propulsion system and recommenda- tions are made for additional research and development</p>	<p>UNCLASSIFIED</p> <ol style="list-style-type: none"> V R. E. Fleeman, L. M. Seal C. Henderson VI. In ASTIA collection VII. Aval fr OTS: \$2.50 <p>UNCLASSIFIED</p>